

REPORT DOCUMENTATION PAGE

Form Approved OMB No. 0704-0188

Public reporting burden for this collection of information is estimated to average 1 hour per response, including the time for reviewing instructions, searching existing data sources, gathering and maintaining the data needed, and completing and reviewing the collection of information. Send comments regarding this burden estimate or any other aspect of this collection of information, including suggestions for reducing this burden to Washington Headquarters Services, Directorate for Information Operations and Reports, 1215 Jefferson Davis Highway, Suite 1204, Arlington, VA 22202-4302, and to the Office of Management and Budget, Paperwork Reduction Project (0704-0188), Washington, DC 20503.

| | | | | |
|---|---|--|--|-----------------------|
| 1. AGENCY USE ONLY (Leave blank) | | 2. REPORT DATE 25-January-2000 | 3. REPORT TYPE AND DATES COVERED Final Report | |
| 4. TITLE AND SUBTITLE Demonstration Tests And An Analysis Of Critical Issues Associated With Low Power TAL | | | 5. FUNDING NUMBERS F61775-99-WE092 | |
| 6. AUTHOR(S) Dr. Alexander V Semenkin | | | | |
| 7. PERFORMING ORGANIZATION NAME(S) AND ADDRESS(ES) TSNIIMASH - EXPORT, JSC 4, Pionerskaya Street Korolev 141070 Russia | | | 8. PERFORMING ORGANIZATION REPORT NUMBER N/A | |
| 9. SPONSORING/MONITORING AGENCY NAME(S) AND ADDRESS(ES) EOARD PSC 802 BOX 14 FPO 09499-0200 | | | 10. SPONSORING/MONITORING AGENCY REPORT NUMBER SPC 99-4092 | |
| 11. SUPPLEMENTARY NOTES | | | | |
| 12a. DISTRIBUTION/AVAILABILITY STATEMENT Approved for public release; distribution is unlimited. | | | 12b. DISTRIBUTION CODE A | |
| 13. ABSTRACT (Maximum 200 words) This report results from a contract tasking TSNIIMASH - EXPORT, JSC as follows: The goal of proposed SOW is to demonstrate current status and performances of low power (0.1...1 kW) Thrusters with Anode Layer (TAL) with using Xenon propellant, provide an analysis of critical issues associated with low power TAL development and potential level of low power TAL characteristics, propose draft of the program for breadboard low power thruster development. | | | | |
| 14. SUBJECT TERMS EOARD, Electric Propulsion, Space Technology, Small Satellites | | | 15. NUMBER OF PAGES 40 | 16. PRICE CODE N/A |
| 17. SECURITY CLASSIFICATION OF REPORT UNCLASSIFIED | 18. SECURITY CLASSIFICATION OF THIS PAGE UNCLASSIFIED | 19. SECURITY CLASSIFICATION OF ABSTRACT UNCLASSIFIED | 20. LIMITATION OF ABSTRACT UL | |

NSN 7540-01-280-5500

Standard Form 298 (Rev. 2-89)
Prescribed by ANSI Std. Z39-18
298-102

**Central Research Institute of Machine Building (TsNIIMash)
TsNIIMash – Export Company**

**DEMONSTRATION TESTS AND AN ANALYSIS OF CRITICAL
ISSUES ASSOCIATED WITH LOW POWER TAL**

2000

Contents

4. Test facility and demonstration test of TAL D-38 and T-27.

| | |
|--|----|
| Introduction..... | 3 |
| 1. The concept and types of Hall thrusters with closed drift of electrons..... | 5 |
| 2. Design and performance of existing TALs | 9 |
| 3. Analysis of factors associated with development of anode layer thrusters of low input power | 13 |
| 4. Test facility and demonstration test of TAL D-38 and T-27 | 20 |
| 5. Discussion | 29 |
| Conclusion | 32 |
| References..... | 33 |
| Appendix..... | 34 |

Introduction

This report presents results of work conducted by TsNIIMASH and TsNIIMASH-EXPORT (Russia) under CONTRACT № F61775-99-WE092 with European Office of Aerospace Research and Development (EOARD).

The report contains an analysis of problems associated with development of anode layer thrusters of low input power and experimental data have been collected using available devices D-55, D-38 and T-27 in input power range from 100 to 1000 W with addition of results of thrusters demonstration testing at TsNIIMASH facilities on October 1999.

Electric thrusters are currently in use for station keeping and orbit correction providing increased life time of a number of electrically propelled spacecrafts [1].

Miniaturization of the onboard electronics should significantly reduce total mass of future spacecrafts (down to 500 kg) and necessary onboard energy capability (down to a few hundreds Watts) resulting in necessity to develop adequate propulsion systems of low energy consumption and electric thrusters of reduced input power (down to 50 ... 200 Watts) as however effective as the available devices normally consuming 0,5... 50 kW [1, 2].

Extremely low energy consumption never looked as an special goal for electric propulsion technology, so that there is no distinct approach to solve this problem.

Development of thrusters of reduced input power is a new task for the electric propulsion technology requiring detail review of all aspects concerning the thruster efficiency.

Demonstration of available TAL performance level together with analysis of possibilities and ways to develop thrusters of reduced input power down to 100 ... 200 Watts is an objective of the work here presented .

The propulsion systems of low energy consumption are expected to perform a wide range of orbital maneuver including orbit rising and correction, drag compensation, station keeping in the Sun-synchronous orbit and satellite orientation. In addition the new market of space communication and the Earth sounding systems poses requirements of cancellation keeping and deorbit of exhausted spacecrafts.

The report contains the analysis of problems associated with development of thrusters of reduced input power using the concept of Hall plasma accelerator with anode layer.

The following initial data were used for the analysis mentioned above:

A designated purpose of the propulsion system is station keeping and orbit correction.

Thruster input power – 100...200 W

Propellant– Xenon

Specific impulse is not strictly limited and may be chosen in the range up to 2000 s under the condition of maximal thrust providing at given input power.

The characteristic thruster life time is about 1000 hours.

The thruster operating mode – periodical runs with duration from a few seconds to tens minutes (within the given life time).

Normal energy consumption of a cathode-neutralizer is not greater than a few percent of the total thruster input power. Therefore an effective operating TAL at input powers in the range from 100 to 200 W should be provided with a cathode-neutralizer consuming only a few Watts. Traditionally used hollow cathodes are not serviceable at such low powers so that currently there is neither design nor firing experience on cathodes acceptable for micro TAL . The problem of creating of economical cathode being a separate one is out the scope of the given note.

It is clear that using of electric thrusters of intently reduced input power is not the only way to develop a propulsion systems of low energy consumption. The imposed propulsive requirements may be met with TALs operating in optimal input power range with properly reduced firing time e. g. in a pulse mode with power supply from any accumulative device providing tolerable average energy consumption. TAL ability to operate in 10 s pulse mode was successfully demonstrated in orbit in the ranges of EPDM program [8]. Surely a pulse operating mode requires additional updating of TAL even optimally ticking in steady state operating mode. This task being a separate one is out the scope of the given note.

1. The concept and types of Hall thrusters with closed drift of electrons

The concept of all Hall thrusters with closed drift of electrons including those with anode layer (TALs) is based on acceleration of ions by self-sustained electric field created in a partially magnetized plasma where cross magnetic field mobility of electrons is significantly reduced. The peculiarity of TAL discharge is that its zone along the magnetic field is limited by conducted structure surfaces with cathode potential applied so that electrons are rejected [2].

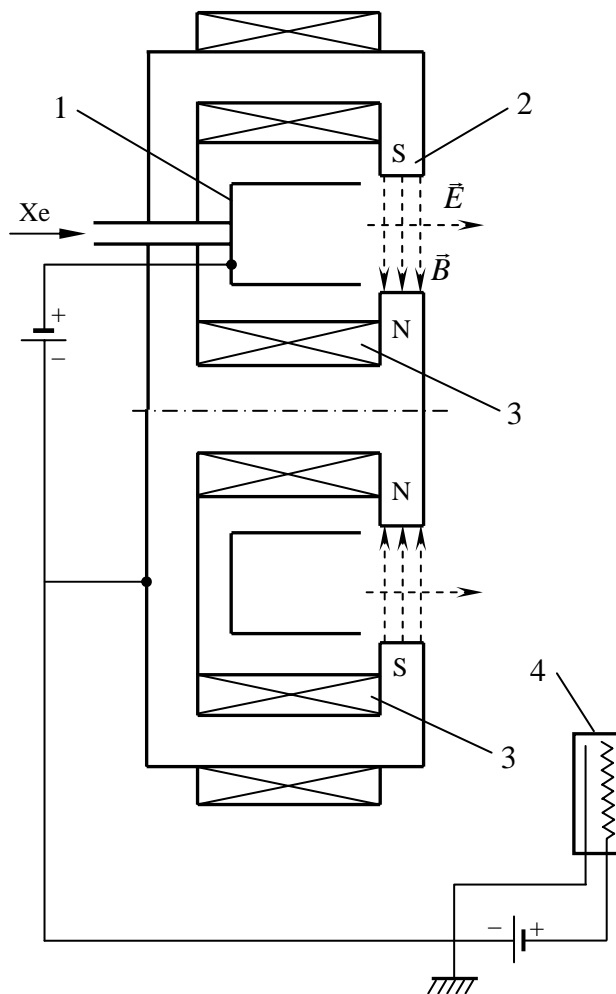


Fig. 1. Thruster with anode layer scheme
1 – anode; 2 – thruster's body; 3 – magnetic coils; 4 – cathode-neutralizer

The following working process is realized in TAL. Gas propellant is fed to the gas distributing ring anode 1 (Fig. 1) where the flow becomes uniformly distributed along the azimuthal direction before it proceeds in the discharge chamber. As a rule the inert gases of great atomic masses are used as a propellant and generally Xe is a preferable choice.

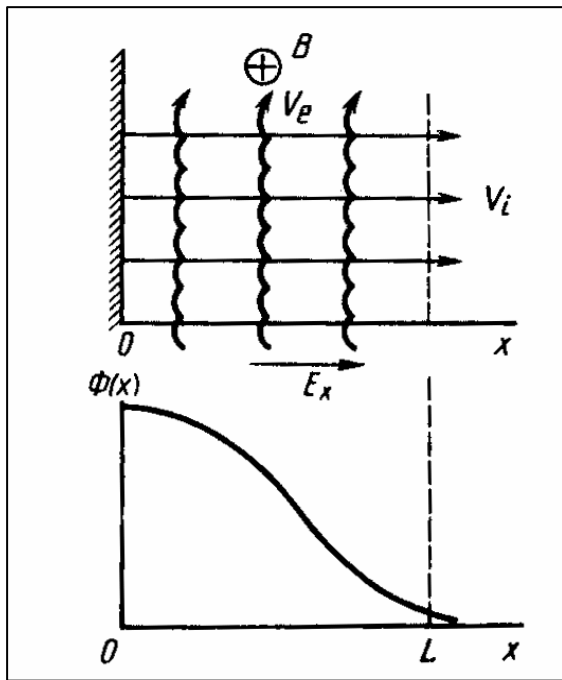


Fig. 2. Distribution of electric potential along electric field.
 V_i , V_e – ion and electron velocities; L – length of anode layer.

The voltage applied between the anode 1 and the cathode neutralizer 4 produces the accelerating electric field E directed perpendicular to the magnetic field B existing between magnetic pole pieces. In the discharge chamber the working gas is ionized and the electric field E accelerates the ions producing reactive thrust. At the thruster exit the accelerated ion beam is neutralized with electrons escaping the cathode neutralizer.

In the magnetic pole pieces gap an azimuthally symmetrical cross field discharge arises with voltage drop from the anode level down to zero at the distance of about few electron cyclotron radiuses. The resulting plasma formation was denoted anode layer. In this anode layer the electrons are being magnetized and azimuthally drifting sometimes collide with the propellant atoms, ionize the latter and as a result jump in the anode direction, i.e. along

E field producing axial current.

Fig.2 shows the voltage distribution along the azimuthally uniform electric layer. Electron mobility along the electric field is strictly limited so that the electric force energizes ions accelerating them in the axial direction. Because low electron mobility across the magnetic field the accelerating zone is narrow enough – not greater than about 1 cm if thruster operating mode is optimal.

It is worth noting that this zone is being usually attached to the positive electrode, may be noticeable shifted away with corresponding choice of the magnetic field distribution profile, however the potential at the high-voltage boundary of EB -discharge is still close to the anode one.

The possibility to regulate axial position of anode layer with proper choice of the magnetic field distribution profile is realized in concept of "external anode layer " allowing to shift the discharge zone outdoor the structure exit plane with corresponding reduction of structure wearing and increase of thruster life time [3, 11].

There are two namely single- (fig. 1) and double-stage schemes (fig. 3) realizing the TAL concept [2]. The double-stage TAL design allows to keep two axially separated anode layers so that the first one serves as a gas ionizer whereas the second stage provides ion acceleration, whereas in single-stage TAL the only existing anode layer provides gas ionization and ion acceleration.

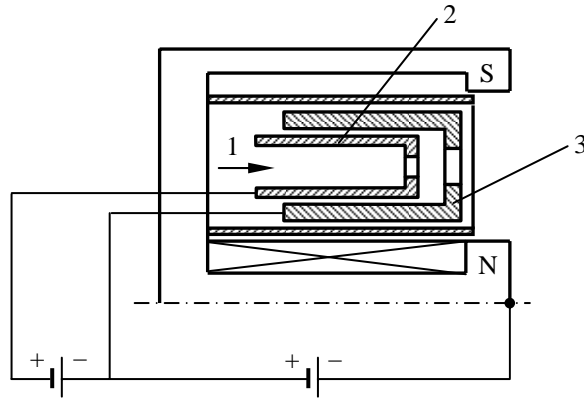


Fig. 3. Double stage TAL scheme:
 1 – propellant flow feed; 2 – the first stage anode;
 3 – the second stage anode

The double-stage TALs are characterized with higher specific impulses in the range of 2500...10000 s whereas the single-stage TALs are preferable in the range of 1000...3000 s. The latter being more simple in design is also perspective for provision of maximal thrust at low input power [1,2,3,5,11].

The concept of "external anode layer" mentioned above is applicable for single- and double-stage TAL schemes both.

TALs conceptually being Hall accelerators with closed drift of electrons, are similar to Stationary Plasma thrusters (SPT) [1].

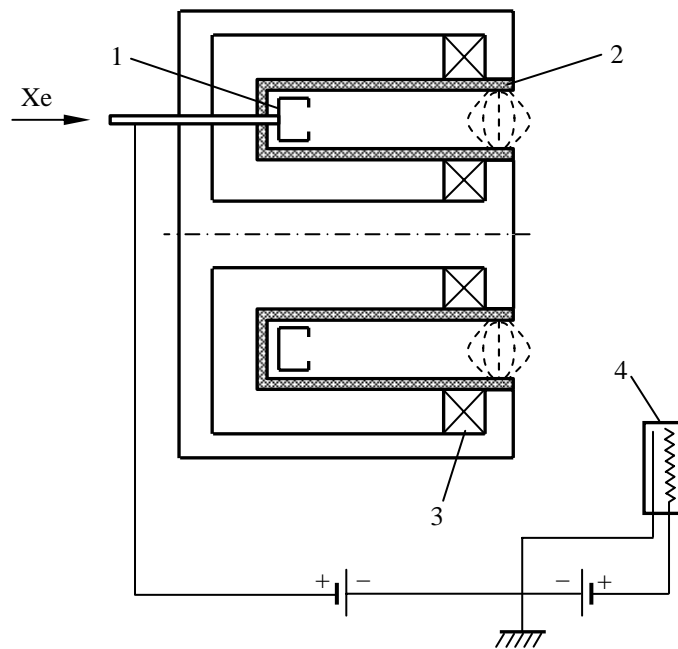


Fig. 4. Stationary plasma thruster scheme:
 1 – anode; 2 – dielectric canal; 3 – magnetic coils; 4 – cathode-neutralizer

Unlike TALs with conductive walls of the discharge chamber, the latter in SPT (Fig. 4) are covered with dielectric materials (ceramics). This structural difference improves working processes in TALs comparing to SPT and also simplifies the thruster structure and technology in total. In addition, the conductive walls of TAL discharge chamber may be made of pyrolytic graphite, the most resistant material against erosion due to bombardment by energetic particles of the discharge plasma.

Due to specific of discharge in TAL, near-wall processes in discharge chamber are not so significant for anode layer thrusters as compared with SPT. Together with relatively low erosion of the thruster parts it leads to several enough important features: stability of the thruster parameters, insensitivity to outer contamination and in turn low contamination of the spacecraft surface, such as solar arrays, optic devices and so on, by sputtered material.

For given operating mode and input power TALs are more compact, less heavy and less noisy in the sense of electromagnetic interference as compared to other electric thrusters [4,6].

2. Design and performance of existing TALs

Recently most of TAL development activity was concentrated on a family of xenon anode layer thrusters with relatively low specific impulse - 1000...2000 sec and nominal range of input power from 0,5 to 50 kW. The reason was wide potential application of such thrusters for different missions - from orbit keeping of the commercial communication satellites to planetary mission.

The available nomenclature set of thrusters with anode layer ,created by TsNIIMash, and their technical characteristics are presented in Table 1 [1].

Table. 1

| Thruster | Power, kW | Specific impulse, m/s | Efficiency, % | Thrust, mH | Propellant |
|----------|------------|-----------------------------|---------------|-------------|------------|
| T-27 | 0,2÷0,7 | $(10 \div 20) \cdot 10^3$ | 50 | 15 ÷ 50 | Xe |
| D-38 | 0,2 ÷ 1,5 | $(13 \div 28) \cdot 10^3$ | 50...70 | 25 ÷ 100 | Xe |
| D-55 | 0,8 ÷ 2,5 | $(13.5 \div 27) \cdot 10^3$ | 55 | 40 ÷ 120 | Xe |
| D-100-I | 1,3 ÷ 7,5 | $(14,5 \div 28) \cdot 10^3$ | 60 | 80 ÷ 340 | Xe |
| D-100-II | 3,5 ÷ 15 | $(18 \div 42,5) \cdot 10^3$ | 65 | 80 ÷ 650 | Xe |
| D-110 | 0,6 ÷ 4,5 | $(10 \div 25) \cdot 10^3$ | 50...60 | 50 ÷ 240 | Xe |
| D-150 | 4,5 ÷ 17,5 | $(15 \div 31) \cdot 10^3$ | 60 | 20 ÷ 800 | Xe |
| TM-50 | 20 ÷ 50 | $(30 \div 70) \cdot 10^3$ | 70...75 | 1000 ÷ 2500 | Xe |

All presented laboratory thrusters are of single-stage design except D-100-II and TM-50 being double-stage schemes. The D-38 and D-55 thrusters have also flight versions.

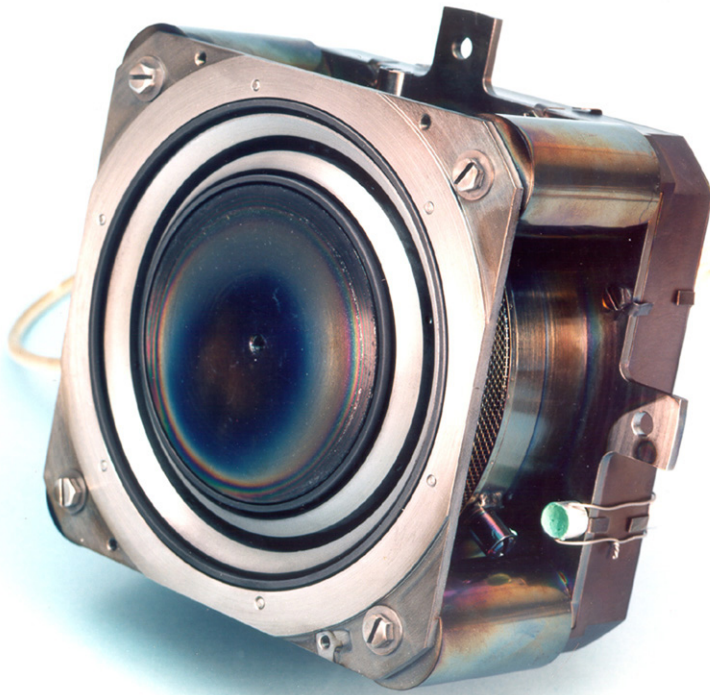
All these thrusters allow regulation in a wide range of parameters.

The general views of a number of some thrusters listed above are shown on a photos Figure 5.

Fig. 6 shows the structural scheme of traditional single-stage thruster with anode layer which includes the following main parts and components:

magnetic system consisting of magnetic body (4) with pole pieces (7), one inner (3) and a few outer coils (5);

- gas-distributing anode ;
- discharge chamber walls ;
- insulators ;
- cathode-neutralizer (not shown).



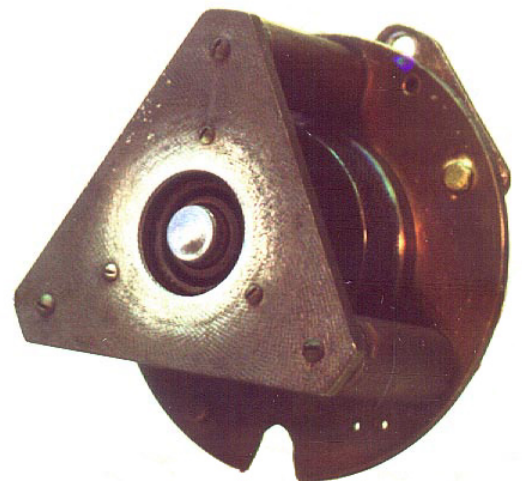
D-110 thruster



D-55 thruster



D-38 thruster



T-27 thruster

Fig. 5. General view of thrusters

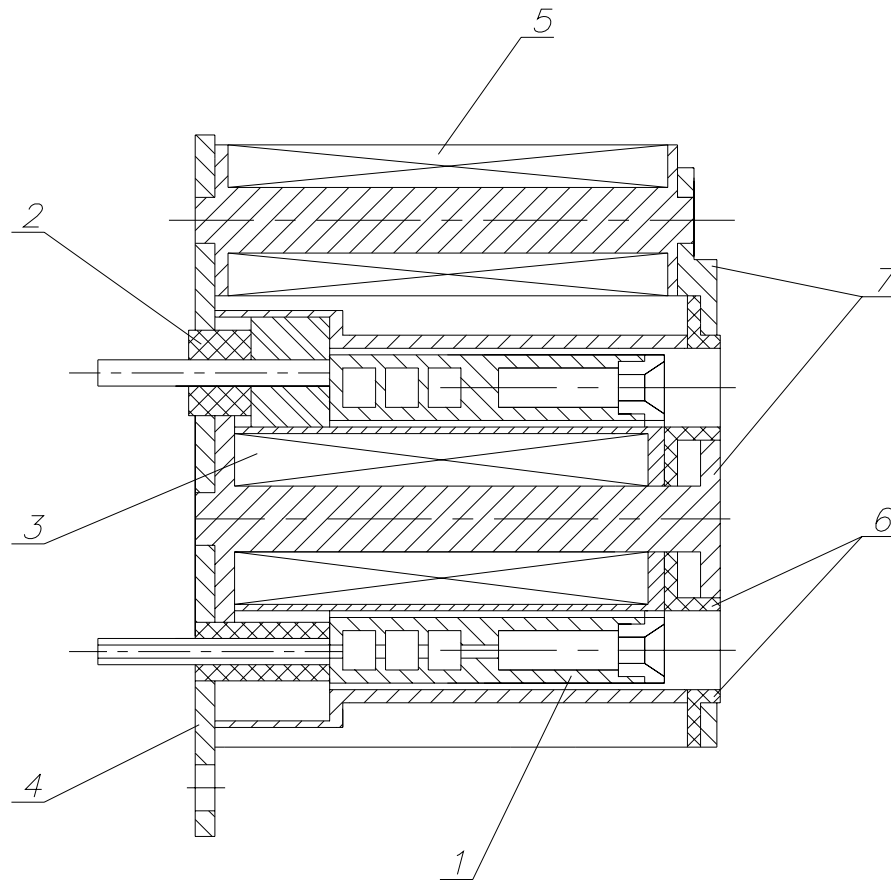


Fig. 6. Thruster design scheme.

The magnetic system applies a magnetic field of desired strength and configuration to the discharge zone.

The use of magnetic coils allows proper regulation of the magnetic field in various operating modes which simplifies the task of thruster optimization. The outer coils connected in series and the single inner coil are powered separately by independent power supplies. The magnetic body (Ref. 4 of Fig.6) is also the load carrying structure, with all other thruster parts and components are being mounted on it.

The anode (Ref. 7 of Fig. 6) is a positive electrode in the discharge chamber and operates as a gas distributor. The working gas is fed into the inner ring cavity of the anode and through the set of holes providing uniform distribution of the propellant in the discharge chamber along the azimuthal direction. The magnetic pole pieces are provided with shields – guard rings (Ref. 6 of Fig.6) protecting the pole pieces from accelerated ion flux incidence and sputtering.

The anode supporting insulators provide its electrical isolation from other parts of the device.

All thrusters of existing nomenclature set are developed using the similar design technology and demonstrate approximately equal efficiency of working process despite significant difference in the characteristic sizes.

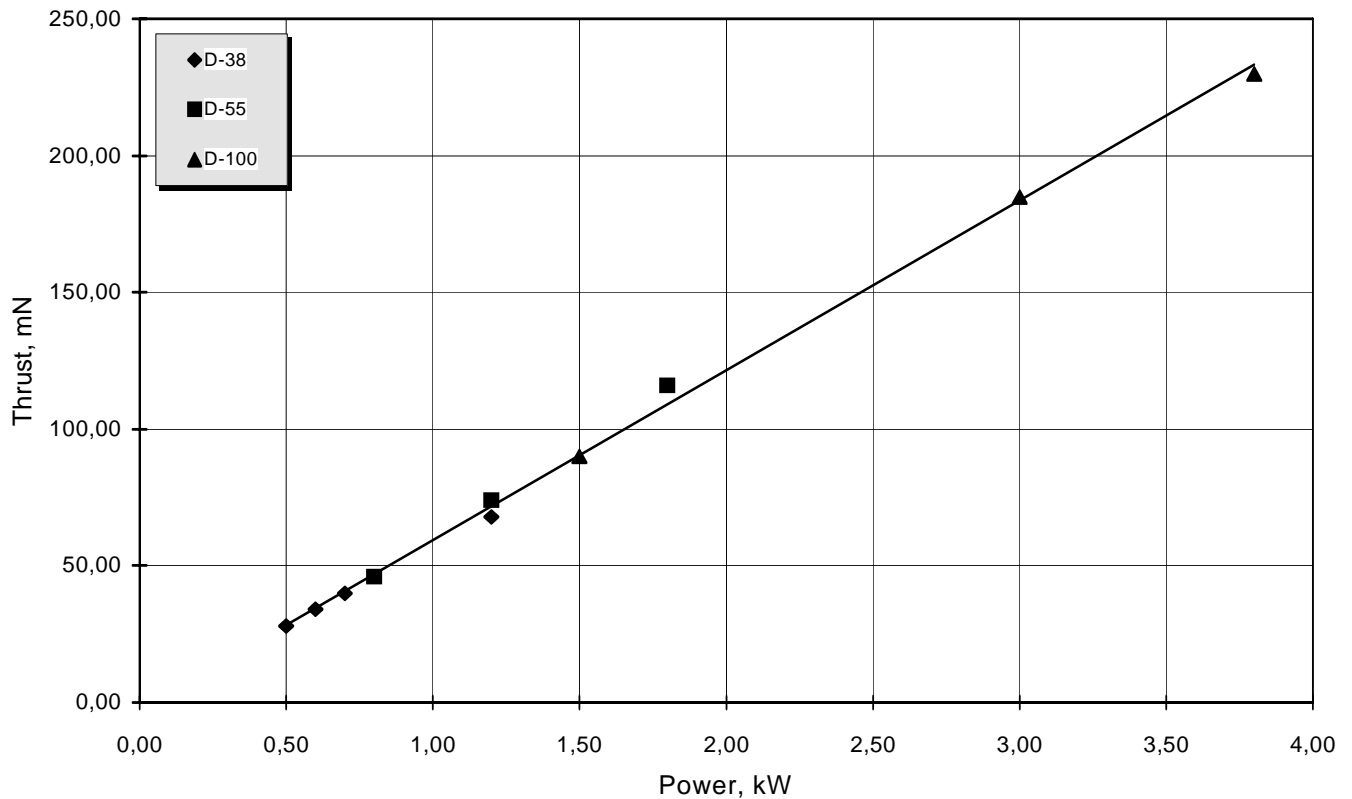


Fig. 7. Linear thrust characteristic.

Fig. 7 suggests that dependence of thrust on input power is linear at a preferable discharge voltage 300 V for several devices tested despite of a change in sizes.

The existing single stage thrusters provide specific impulses in the range from 1000 to 2500 s with maximal obtained efficiency up to 0,6...0,7.

Several thrusters namely D-38, D-55, D-100, TAL 110, TM-50 underwent a detail study at leading research centers of the USA [4,7,9] and D-55 thruster was used as a base for development of flight version TAL-WSF successfully tested onboard STEX spacecraft in the ranges of EPDM program during October 1998 – March 1999 [8].

3. Analysis of factors associated with development of anode layer thrusters of low input power

The main existing bulk of data on TAL design and performances is collected for the range of input powers from 0,5 to 50 kW, and the available experience shows that no essential changes in thruster behavior occur over this wide range of operating conditions.

In contrary to this trend, with decreasing of input power and thruster structure dimensions some scale factors should impact TAL working process and performance.

Since the existing TAL devices were designed to operate at higher input powers than those specified in the Contract, the performed works were advanced in three main directions:

- experimental demonstration of characteristics of the existing TAL devices at lower than designed input powers,
- analysis of physical and technical factors limiting possibility to develop highly effective anode layer thruster for operation at low input powers,
- evaluation of possibility to create a special TAL version for operation at input powers in the range from 100 to 200 W

The available understanding in physical mechanisms of TAL operation and the experience in TAL operation suggest that there are two ways to decrease input power of TAL:

- Decreasing of the discharge voltage,
- Decreasing of the anode mass flow rate and the discharge current.

Both possibilities have inherent natural limitations. Let us to consider this in more details.

Fig. 8 shows a typical Volt-Ampere characteristics of a single stage thruster with anode layer. On this curve there are two distinct ranges where discharge current depends on discharge voltage quite differently. Operating mode, named as "accelerating" one, relates to the region of nearly constant discharge current. This operating mode is the most effective and the ion beam is properly focused. With decreasing of the discharge voltage below the threshold, V^* , the current begins to rise and the thruster transits to "anomalous" operating mode characterizing with enhanced oscillations and lower efficiency whereas the ion beam is non-focused.

Although the nature of this transition to "anomalous" operating mode is not still quite clear, the threshold V^* puts the lower bound of tolerable decreasing of the thruster input power using regulation of

discharge voltage, since the minimal power to thrust at given input power may be obtained only within the "accelerating" operating mode.

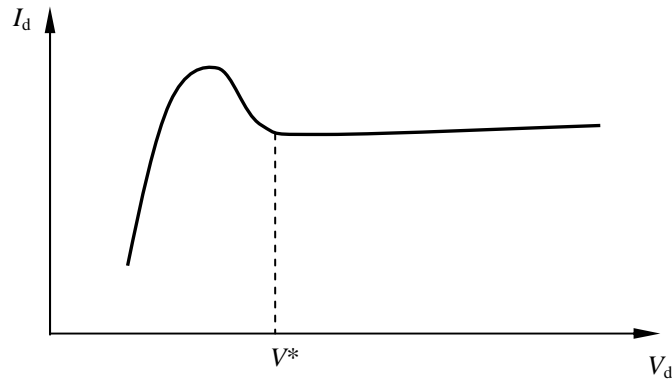


Fig. 8. TAL Volt-Ampere characteristic.

For the thrusters with anode layer the characteristic values of V^* relates to the range from 100 to 200 V depending on the thruster design and operating mode established.

The second way to decrease input power of TAL with lowering of the anode mass flow rate and the discharge current is also characterized with its inherent limitation since the mass flow density, j , in the discharge region must meet requirement $j > j_a$, the minimal value providing propellant ionization effective enough, where

$$j_a = \frac{e^2 \cdot B \cdot \sqrt{4 \cdot k \cdot T}}{M \cdot \sqrt{(m \cdot \langle Q_{ea} \cdot v_e \rangle) \cdot \langle Q_i \cdot v_e \rangle}},$$

where

E is electron charge,

B is average value of magnetic field,

M is ion mass,

Q_{ea} is cross sectional area of electron-atom collisions,

Q_i is effective cross sectional area of ionizing collisions,

v_e is electron velocity.

According to this expression the mass flow density of Xenon in the discharge region must be kept greater than approximately $0,1 \text{ A/cm}^2$.

So that input power of TAL can not be arbitrary decreased with no penalty in thruster efficiency and that also there is necessity to minimize thruster structure dimensions to keep high ionization

efficiency .

The average anode diameter is parameter generally characterizing operating range of a thruster, will be further used as the main parameter for thruster type classification.

Let us examine the main factors impacting TAL working process, performance and design while decreasing thruster size and input power (below 1 kW).

While developing TAL of low input power, two main prerequisites must be taken into account.

Firstly for all design versions the mass flow density in the discharge region must meet requirement $j > j_{min}$, where j_{min} is the minimal value providing propellant ionization effective enough. This results in choice of the average anode diameter and cross-sectional area of the propellant flow channel reduced with reducing of thruster input power.

Secondly the optimal working process may be established only with proper choice of the discharge chamber geometry, value and distribution of magnetic field in discharge zone .

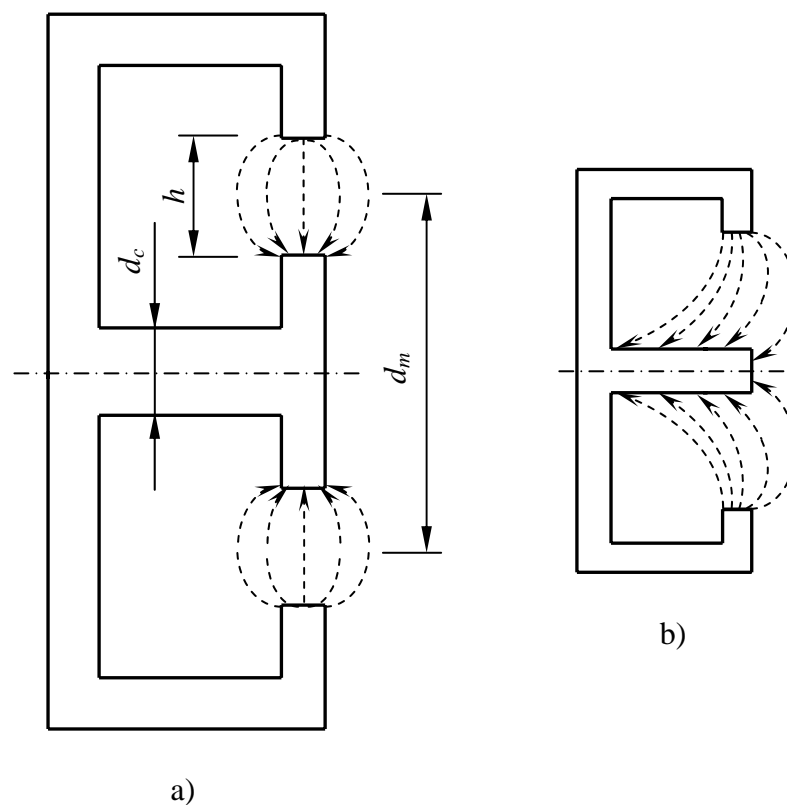


Fig. 9. Schemes of traditional (a) and microTAL (b) magnetic system.

The latter leads to several specific factors.

While proceeding in decrease of d_m , the proper choice of diameter of the central magnetic body core d_c , should follow the dependence, $d_c \sim d_m^{1/2}$, in order to provide desired magnetic induction flux in

the discharge region. Therefore the average anode diameter and the gap between the pole pieces can not be changed in tact multiplying hindrances in decreasing of the thruster input power.

Fig.9 illustrates how may change spatial picture of magnetic force lines distribution from traditional lens geometry to that of defocusing shape, as expected trend with decreasing of the average anode diameter d_m .

An existed natural radial inhomogeneity of the magnetic field value may additionally impact the TAL operating process .

Fig.10 shows a distribution of the value of the radial magnetic induction over the gap between the pole pieces, i. e. in the discharge region. The radial difference in magnetic field value leads to changes of electric fields structure (Fig.2) for different location between magnetic poles.

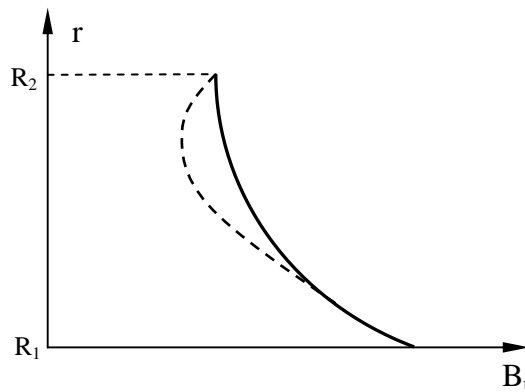


Fig. 10. Radial distribution of magnetic field value.

Such variation arises additional electric field, which is perpendicular to the field accelerating the ions along discharge chamber. It is quite clear that with decreasing of the average anode diameter whereas the gap between the magnetic pole pieces, (R_1-R_2) , are reserved almost constant, the radial inhomogeneity of the magnetic field tends to grow causing additional beam defocusing with corresponding penalty in the thruster performance.

For low power thrusters one can expect increasing of boundary effects causing reducing of efficiency as compared with existing TAL. For example, decreasing of discharge voltage results in ion beam defocusing with corresponding increase of portion of ion flow bombarding the discharge chamber walls [10,11,12].

Along with general physical tendencies there are some technical limitations which are significant while decreasing of thruster size.

Generally there are two ways to provide lifetime of Hall thrusters . The first one is using of special screen protecting the magnetic system from sputtering by accelerated ion beam. Time of erosion of such screens limits thruster life time, and it have to be thick enough to provide required life value.

The second one and of most effective way to minimize erosion of discharge walls and provide life time of Hall thrusters is proper choice of magnetic field distribution over the discharge zone. This way is ultimately realized in the concept of "external anode layer" eliminating straight accelerated ion beam incidence on any structural parts of the thruster [11].

In order to establish the desired distribution of magnetic field over the discharge zone, more sophisticated magnetic systems than that shown in Fig. 1 are to be used e.g. multi polar ones or provided with magnetic screens, see Figures 11a and 11b [13,14].

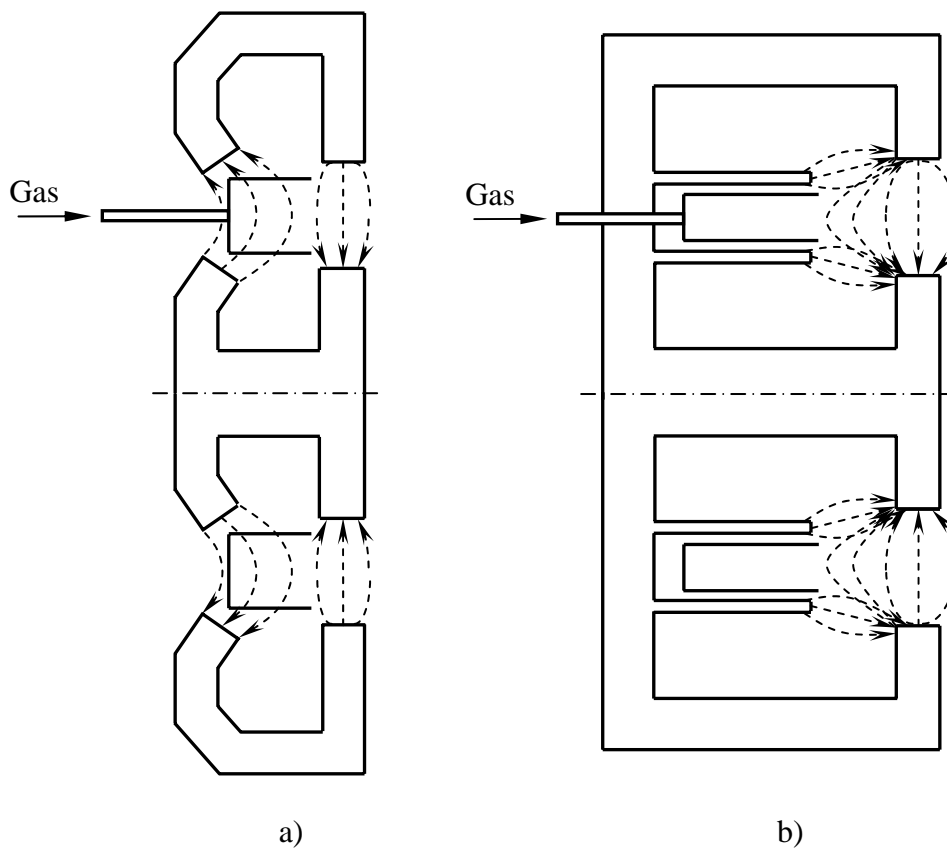


Fig. 11. Multi polar magnetic system and system with screens.

The perspectives to realize magnetic structures of such kind are strictly limited for thruster with small size.

Concerning the problem of thruster life time increasing and basing on the experience available one can characterize the expected relation between the life time and thruster dimensions with the scheme of Fig. 12 displaying three regions of design parameters.

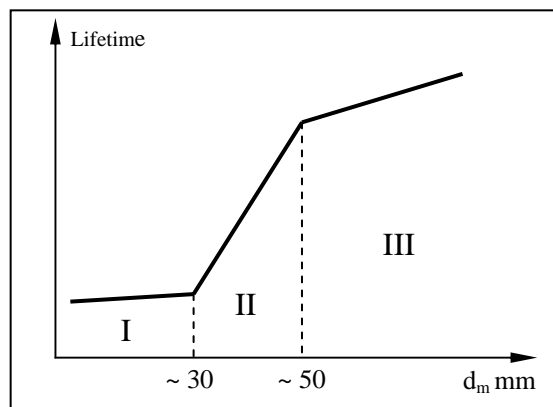


Fig. 12. Life time of thruster.

In region III the thruster size allows to realize the concept of "external anode layer" increasing thruster life time since expected erosion of the pole pieces guard rings is minimal. Increase of thruster dimensions may be accompanied with some grow of life time since allows to make the guard rings thicker and increases the time of their wearing.

In region II the concept of "external anode layer" may be realized only partly. The smaller thruster, the lower opportunity to realize this concept. Thruster design variations in this region may result in dramatic change of expected erosion rate and life time.

In region I the concept of "external anode layer" can not be realized at once so that the thruster life time depends predominantly on thickness of the shields being strictly limited in smaller thrusters.

Fig.3 (see region II) suggests that specially shaped magnetic systems are non-usable for thrusters with average anode diameter lesser than 30...50 mm with input power range of 1...0,5 kW. Nevertheless it is reasonable to expect that the specified life time value of 1000 hours for thrusters of low input power may be provided with no special shaping of the magnetic field. It is worth noting that evaluated life time of the thruster with average anode diameter of 55 mm at input power of 700 W is greater than 3000 hours with no special shaping of the magnetic field [11]. Erosion rate for graphite guard ring at that thruster was about 1 mkm/hour. For the same density of xenon mass flow expected erosion rate decreases approximately proportional to applied discharge voltage. So that to get required life time 1000 hours at 125 V it is enough to have thickness of the graphite ring about 0.5 mm. Obviously that such small value requires small space in the thruster discharge chamber and does not provide any problems for the thruster design. At the same time such thruster parts can be easily manufactured with using existing technologies, and its operation in the thruster is not accompanied with any specific effects - like local overheating, thermal shock cracking and so on. For example, graphite guard rings with thickness 1 mm many times were successfully used in various thruster with anode layer.

At the bottom line of the discussion presented above let us resume the main factors to be taken into account while decreasing input power of thruster with anode layer:

- decreasing of the thruster size leads to non optimal magnetic system geometry and field profile, which cause defocusing of accelerated ion flow and reducing of thruster efficiency,
- an existed radial inhomogeneity of the magnetic field enhances and additionally impacts the thruster operating process especially for small size thrusters,
- the smaller discharge chamber the greater role of edge effects at boundary between plasma and the chamber walls enhancing energy losses to the structure,
- design solutions providing minimal erosion of the structure and maximal thruster life time at high input powers are not applicable for small thrusters.

Being not critical for the traditional operating range of TALs, most of these scale factors never were specifically evaluated in past. For example, many of problems connected with low power TAL elaboration are determined by ionization processes. This problem has been successfully resolved for existing thrusters designed to operate at high input power and propellant density. Potentially the thruster may be modified to get effective ionization at low power and mass flow, but it requires specially dedicated research program, which is out of current efforts.

Big portion of considered scaling factors can not be quantitatively estimated based on available mathematical methods and computer codes, and dedicated experimental study is necessary to get information of boundary limits. So that, in the reported work significance of considered scaling factors for low power TAL was estimated based on existing experimental data obtained on D-55, D-38, and T-27 thrusters and data of demonstration tests of D-38 and T-27, performed under SOW for this Contract.

4. Test facility and demonstration test of TAL D-38 and T-27.

Two TsNIIMash vacuum chambers of 5 and 11 cubic meters equipped with 5 oil diffusion pumps each and with forvacuum mechanical pumps were used to run the thrusters. The general view of the test facility with measuring equipment is shown in Fig.13.

Both vacuum tanks are equipped with identical power supply and xenon management systems and measurement equipment.

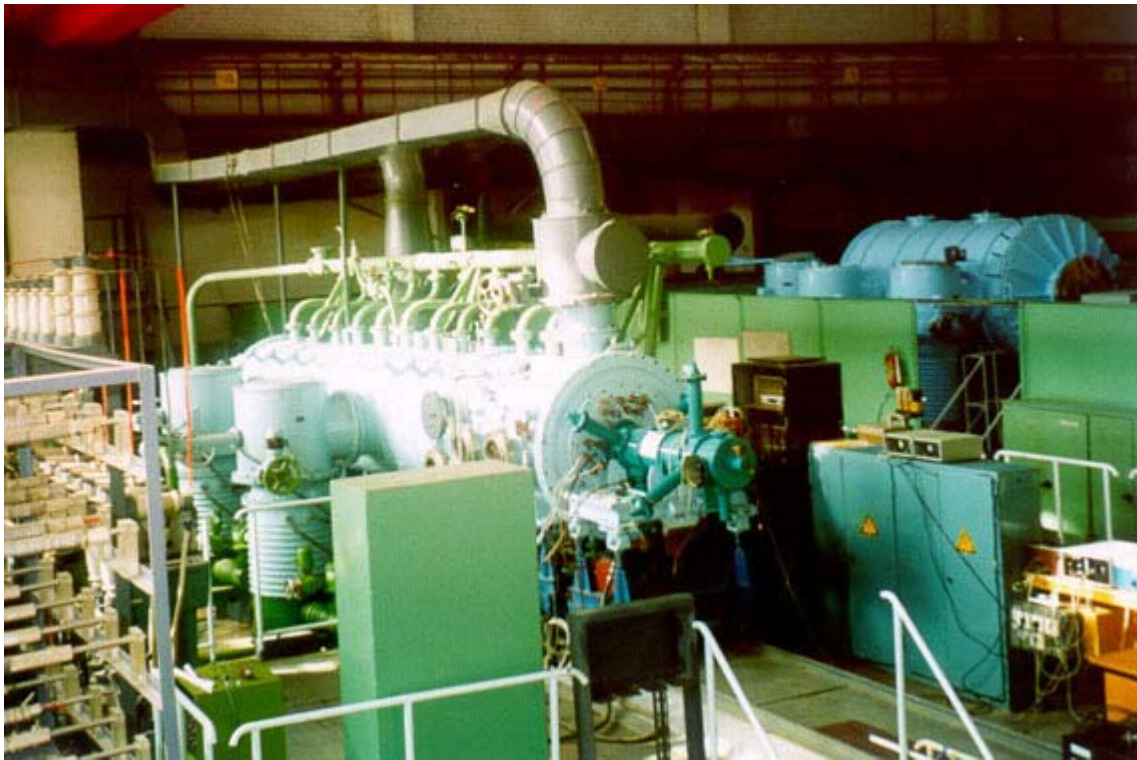


Fig. 13. External view of stand base.

The power supply and control system consist of:

- control panel of the power supply and Vacuum systems;
- a set of *DC* supplies to energize thruster anode, cathode-neutralizer and magnetic coils circuits
- a set of *AC* supplies to energize measuring and accessory equipment

The schematic diagram of the thruster power supply system with electric measuring equipment is shown in Fig.14.

The used *DC* discharge power supply is controllable three-phase rectifier with *LC* filter ($L=15$ mH, $C=50$ mcF) dumping oscillations of the output voltages to the levels less than 6%. The thruster

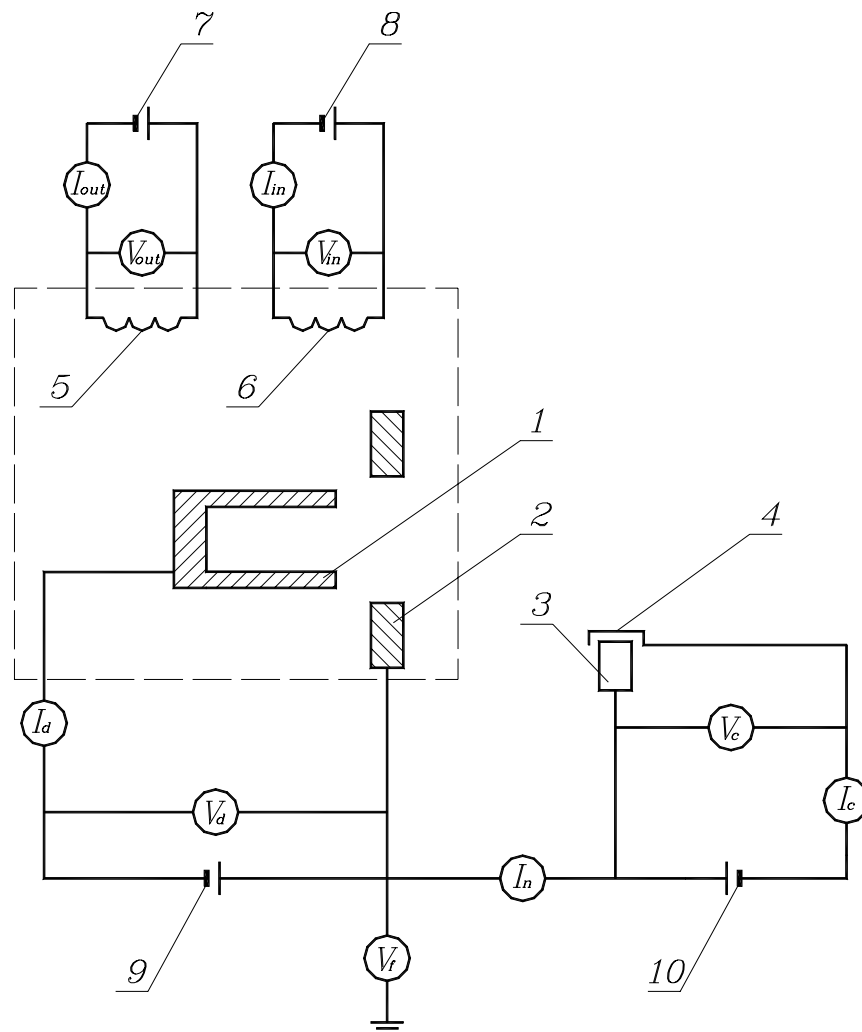


Fig. 14. Thruster electric scheme.

1– anode, 2– magnetic poles, 3– cathode-neutralizer, 4– keeper electrode, 5, 6 – magnetic coils, 7, 8– magnetic coils power supply, 9, 10 – discharge and cathode power supply

discharge circuit includes a ballast resistor, $R=25$ Ohm, limiting circuit current pulses during occasional arcing and shorting. The value of the accessory condenser, C , shunting the discharge gap is 100 mcF.

The thrusters have been tested with TsNIIMash Xenon multi-purpose laboratory hollow cathode providing electron current from 3 to 10 A.

The cathode-neutralizer power supply provided ignition of start up cathode discharge at voltage up to 1000 V and maintenance of the auxiliary discharge with current of 3...4 A inside cathode cavity at voltage 15...20 V.

While operating the thrusters at low input powers, the auxiliary discharge inside cathode cavity was being kept permanently so that the cathode steady state operation mode did not depend on the thruster discharge presence.

Inner and outer magnetic coils were supplied each with independent current stabilized power supply providing controllable output current within a regulation range from 0 to 10 A.

Voltage and current measurements in all circuits namely of the thruster main and the cathode-neutralizer auxiliary discharges as well as of the magnetic coils one were taken using digital instruments. All meters and measuring circuits had been beforehand calibrated using special calibration instruments of 0,5 accuracy class according to the Russian standard.

The propellant management system included two independent feed line for the thruster anode and the cathode-neutralizer correspondingly.

Xenon mass flow rate was regulated manually using a fine leak valve.

Flow rate values were determined using a constant volume technique based on measuring of climb speed of a liquid driving a known volume (here 10 ccm) of a supplied gas out a glass tube with a scale here marked in 0.1 ccm.

The time of the tube filling with the liquid was measured using a stopwatch with the scale factor of 0.1 s. The indicated value is an average of 2 – 3 readings.

The mass flow rate value was calculated as:

$$m_a = 1,36 \cdot 4,3 \cdot \frac{10 \cdot T_0 \cdot P}{T \cdot P_0 \cdot \tau},$$

where

P_0 is the normal atmospheric pressure (760 Torr)

P is the current atmospheric pressure inside the measuring tube at the time of reading

$T_0 = 273$ K

T is the gas temperature

τ is the time of the measuring tube filling with a liquid

The thruster equipped with a cathode-neutralizer was mounted to a pendulum style thrust measuring device using automatic compensation of the measured force with direct feedback.

The thrust value was calculated according to the relationship:

$$F = (A/A_0) \cdot F_0$$

where A is a difference of output thrust stand signals for switched on and off thruster, A_0 is the output signal value of the thrust stand being loaded with the calibrated weight and F is the calibrated weight value.

Before a test run thruster's circuitry insulation was examined and the thruster was remained at vacuum level of 10^{-1} - 10^{-2} Torr for at least 8 h allowing the structure to outgas.

At every operating point before any reading to perform a 5-10 min lag was made allowing the thruster to achieve steady heat state.

Also at every operating point magnetic coil currents were optimized on criterion of minimal discharge current I_d . Every measurement was repeated at least 2 times for better statistics.

Demonstration tests were performed using TsNIIMash D-38 and T-27 thrusters. Both thrusters, as well as all TAL set shown in the Table 1, are based on one and the same design scheme (see Fig. 6).

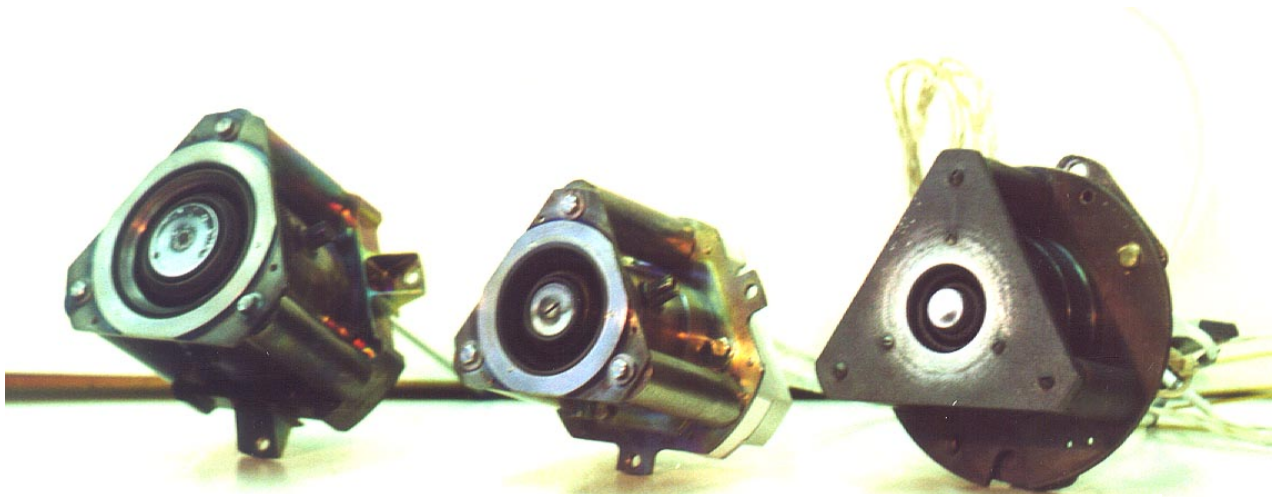


Рис. 15. General view of D-55, D-38, T-27 thrusters (from left to right).

The thrusters general view is shown in Fig.15. D-55 thruster, used for comparison of the thrusters performances, is shown also (left one on Fig.15).

The D-38 thruster is a flight prototype version for Module-M flight experiment [3], whereas the T-27 thruster is a ground laboratory version designed for technological use.

The thrusters both were designated to operate at higher input powers than 100...200 W range of interest. Partially the D-38 thruster was designed to consume 750 W at specific impulse 2200 s with ability to be reinforced up to 1500 W. The T-27 thruster was designed to operate in 300...1000 W input power range.

During the demonstration tests a performance characterization of the thrusters was accomplished over 50...500 W range with an emphasize to that of 100...200 W specified in the Contract. Discharge voltage was varied over 100...300 V range where thrust to input power ratio is expected to be maximal. The lower border of the discharge voltages tested was put by thruster transition to the "anomalous" operating mode characterized with enhanced plasma oscillations and ion beam defocusing.

Energy expenses in the magnetic coils and cathode-neutralizer as well as gas flow rate through the latter were not taken into account while calculating the thruster efficiency and other characteristics.

Test results are presented in Appendix 1.

Being shown in Figures 16-19, typical dependencies of thrust, specific impulse, power to thrust ratio and efficiency on Xenon flow rate and discharge voltage for D-38 and T-27 thrusters illustrate general performance features of the thrusters with anode layer namely efficiency grows with increasing of propellant flow rate and existence of optimal discharge voltage range (here 100...150 V), where power to thrust ratio is minimal, and its value is about 145 W/Gram for both thrusters. As it was mentioned above, effective thruster operation at minimal discharge voltages depends on boundary between “acceleration” and “anomalous” modes. Such boundary for tested D-38 and T-27 was at 100V and 125V correspondingly. Should be noted that no special efforts were made to adjust the hardware for operation at minimal voltages and the thrusters were taken as it is.

Two typical zones may be specified on the dependencies of efficiency versus mass flow. At low mass flows – near the boundary of effective ionization - thrust efficiency grows up significantly with increasing of Xenon flow. With further increasing of mass flow efficiency value reaches the upper limit and is approximately constant. At the latter regimes the thruster reaches maximum of propellant ionization and thrust value is proportions to mass flow with good accuracy. So that such regimes should be considered as optimal one for particular thruster.

For fixed 155 W operating mode the T-27 thruster exposed the best efficiency of 0,35 with thrust 1,05 g at specific impulse 1085 s. At input power 214 W the efficiency was risen to 0,41 with increase in thrust up to 1,37 g and in specific impulse to 1347 s.

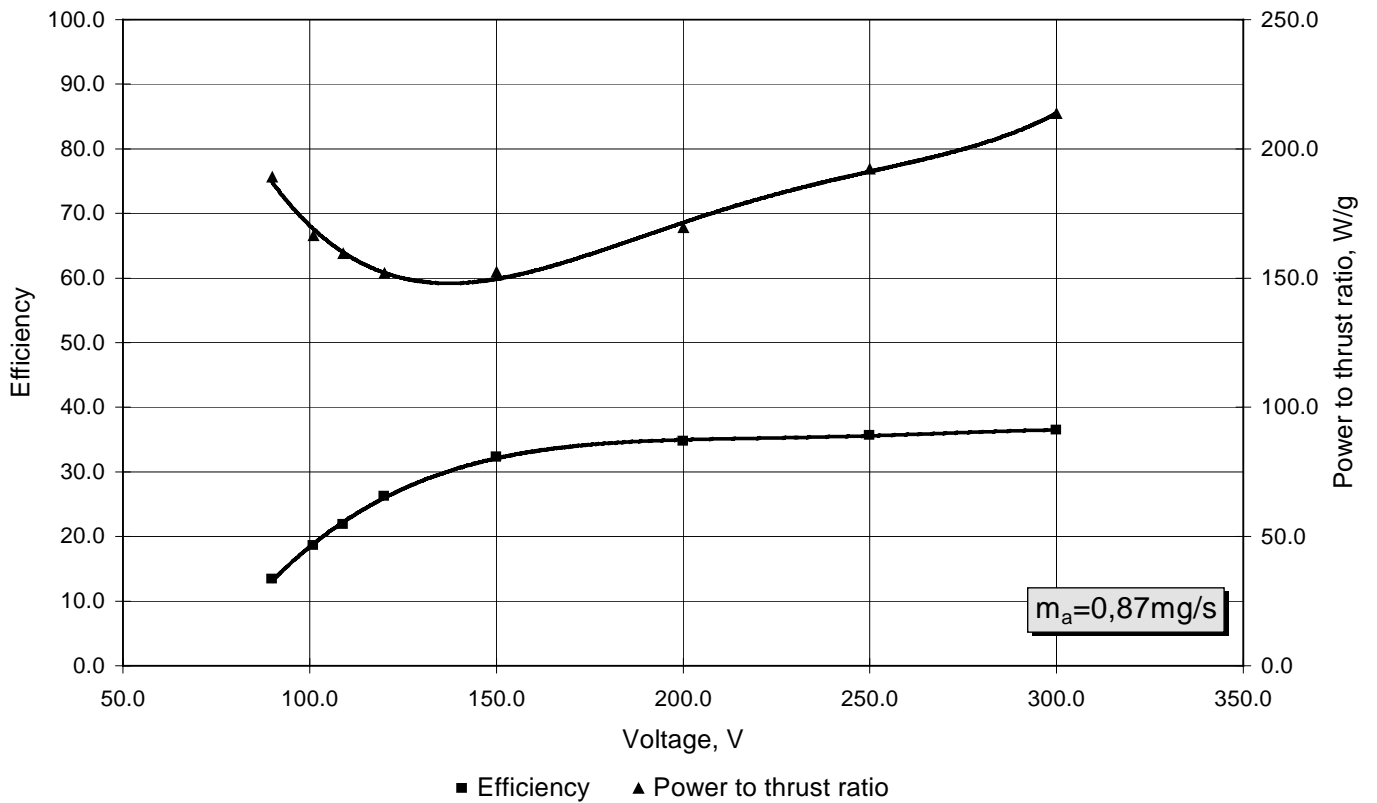
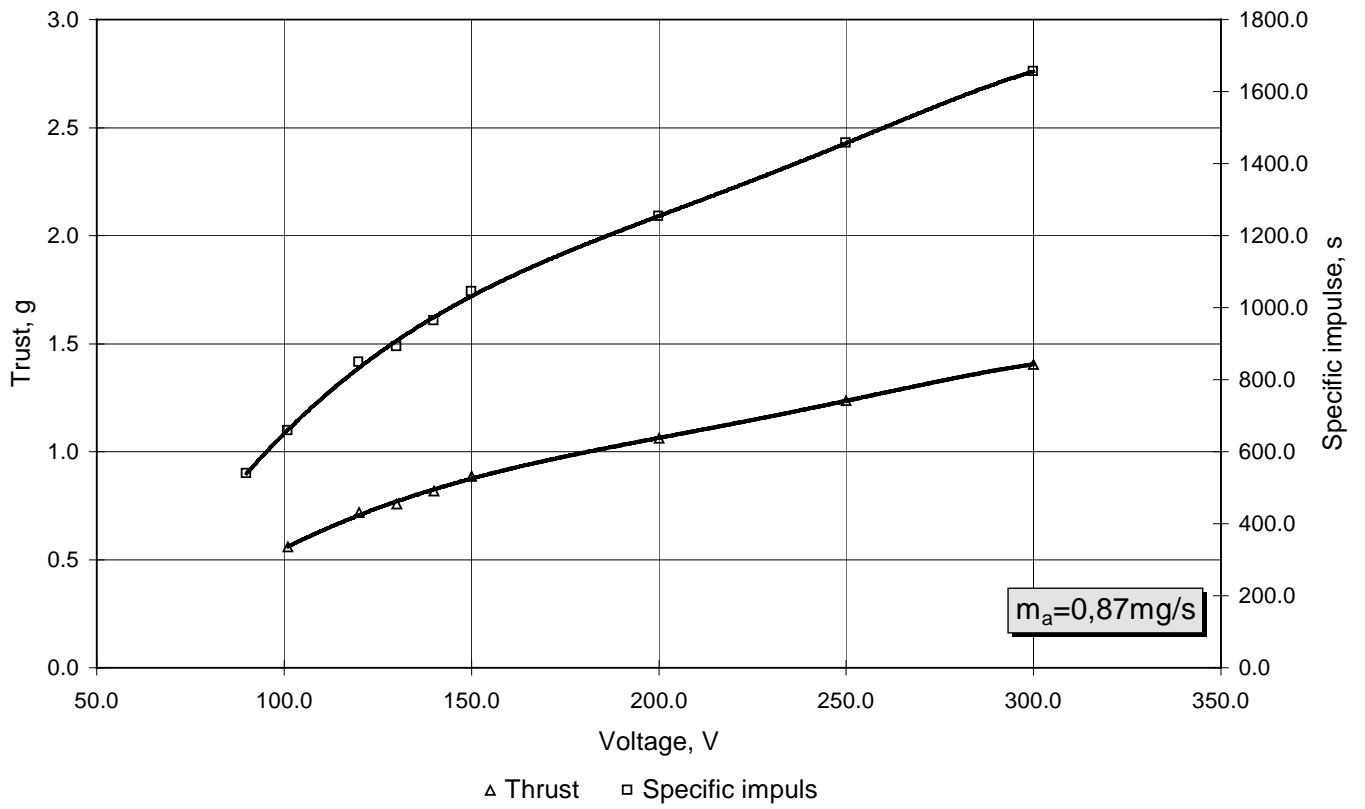


Fig. 16. Performances of T-27 thruster versus discharge voltage.

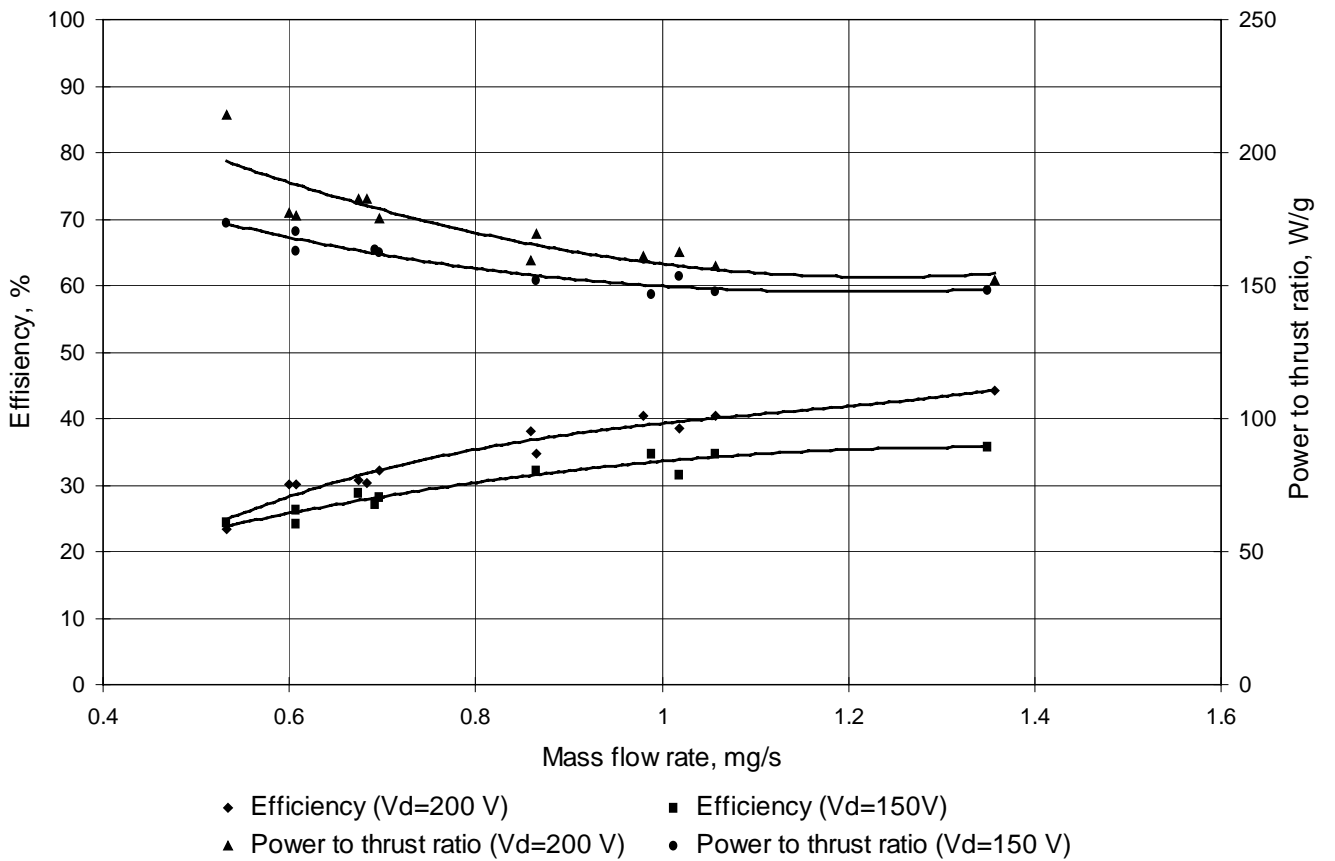
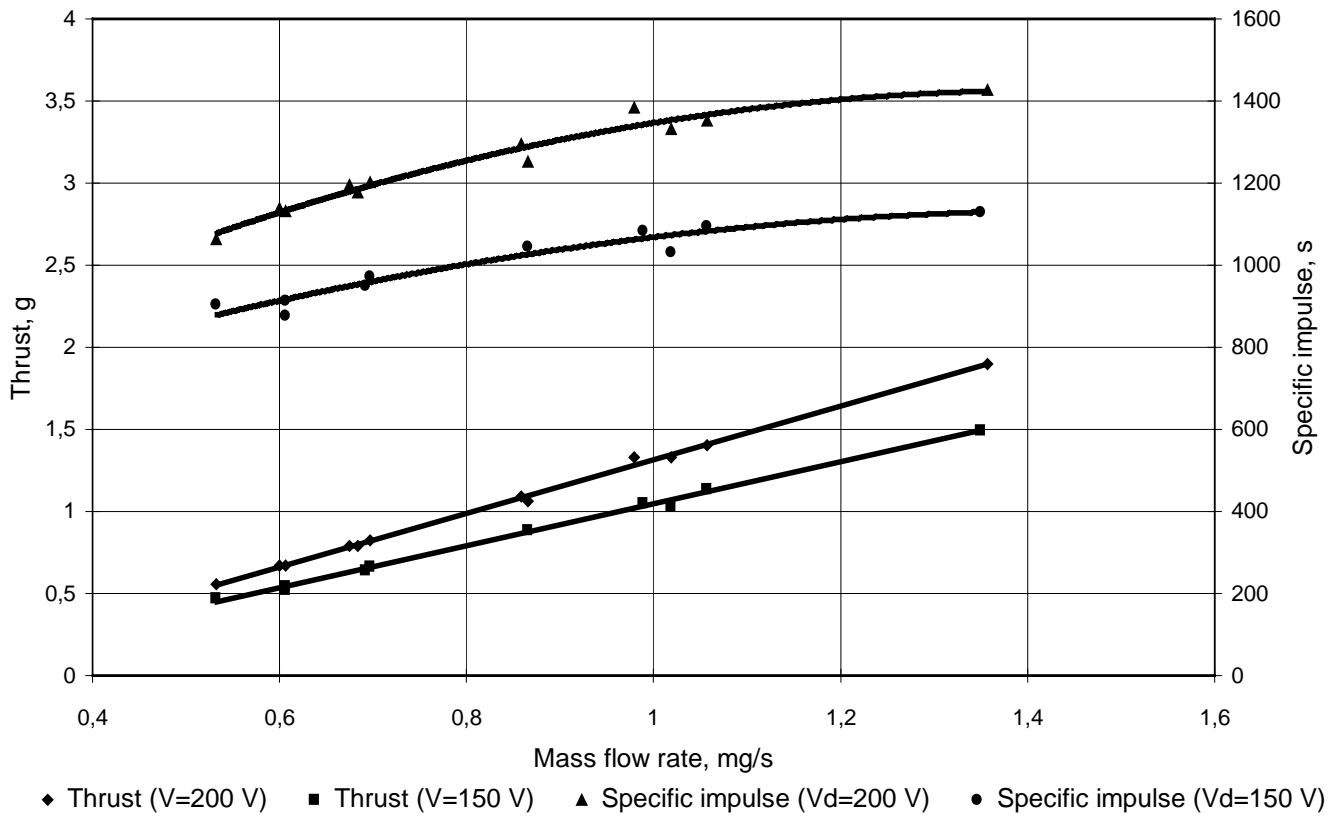


Fig. 17. Performances of T-27 thruster versus mass flow rate.

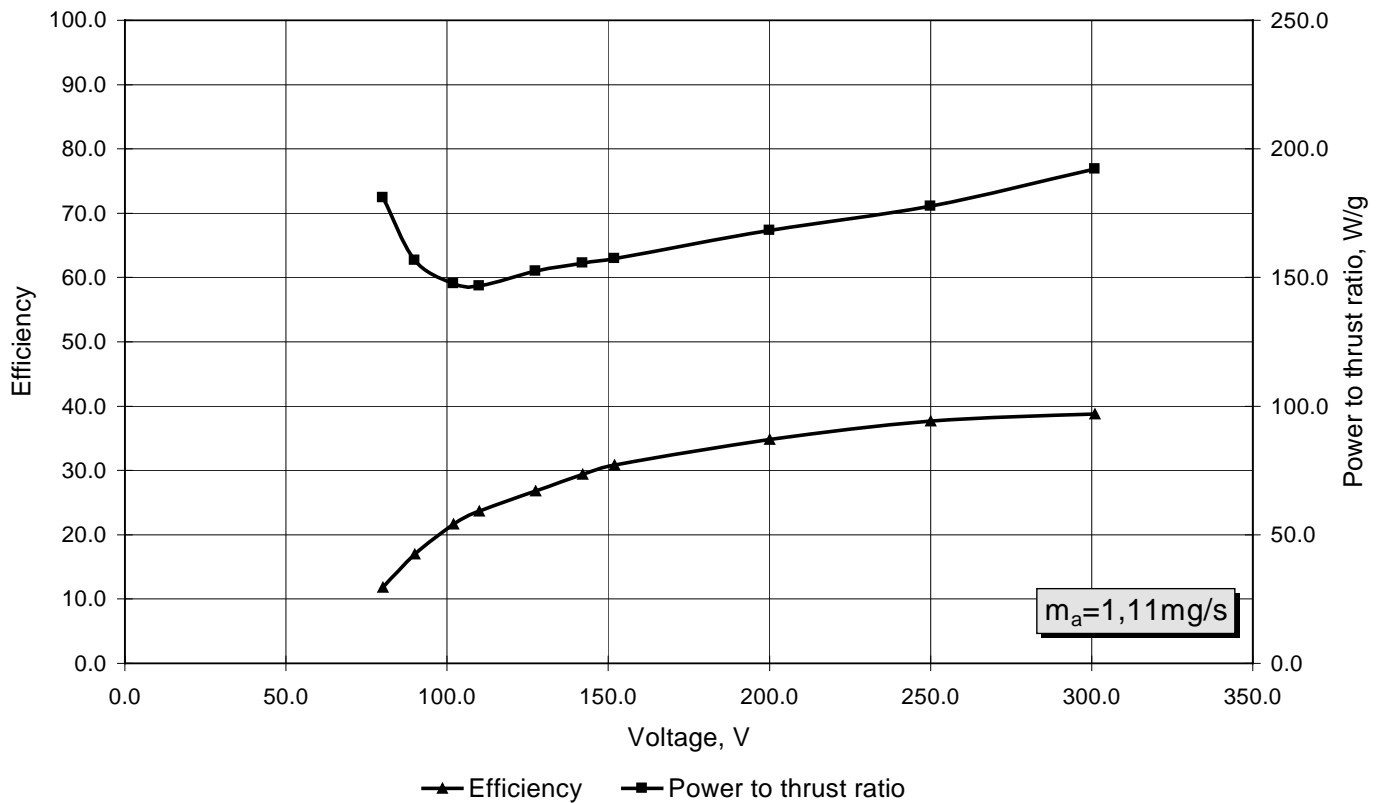
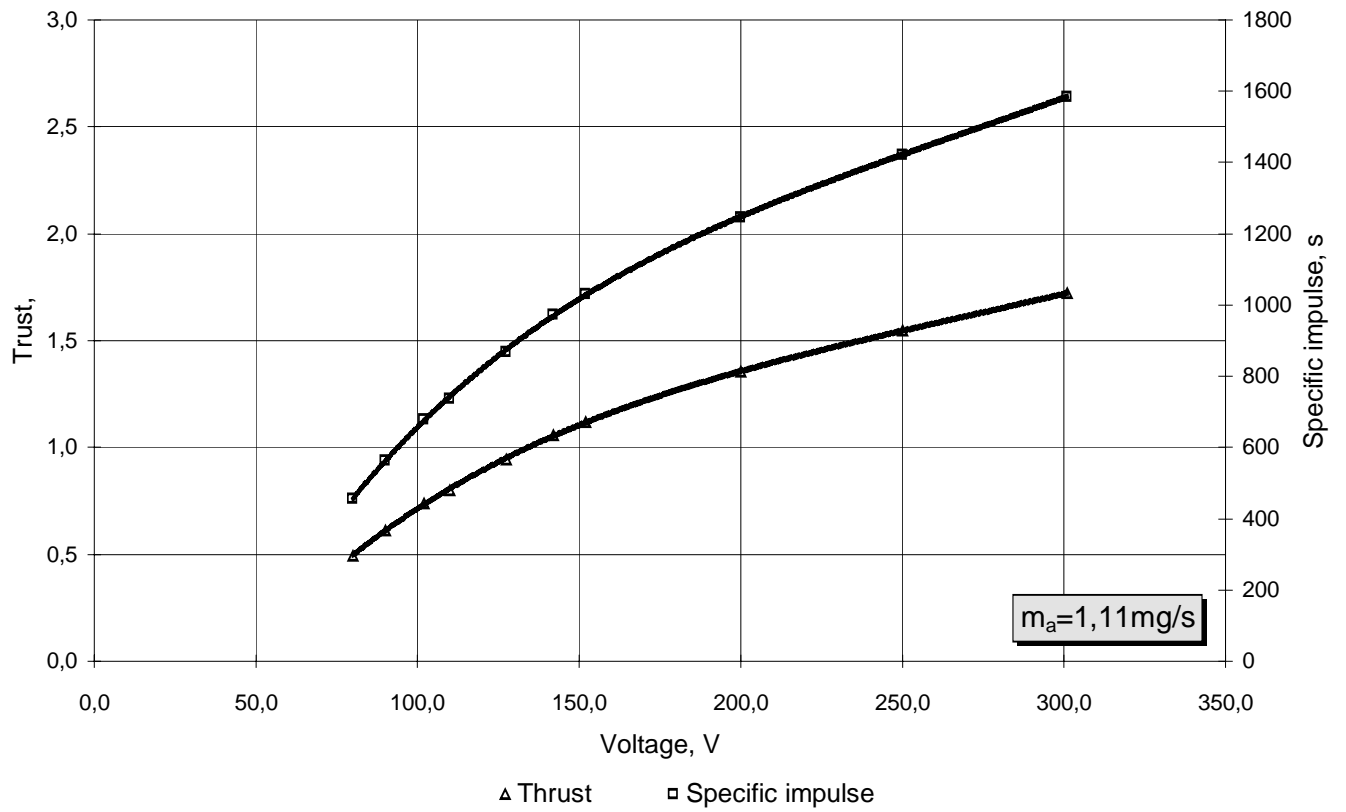


Fig. 18. Performances of D-38 thruster versus discharge voltage.

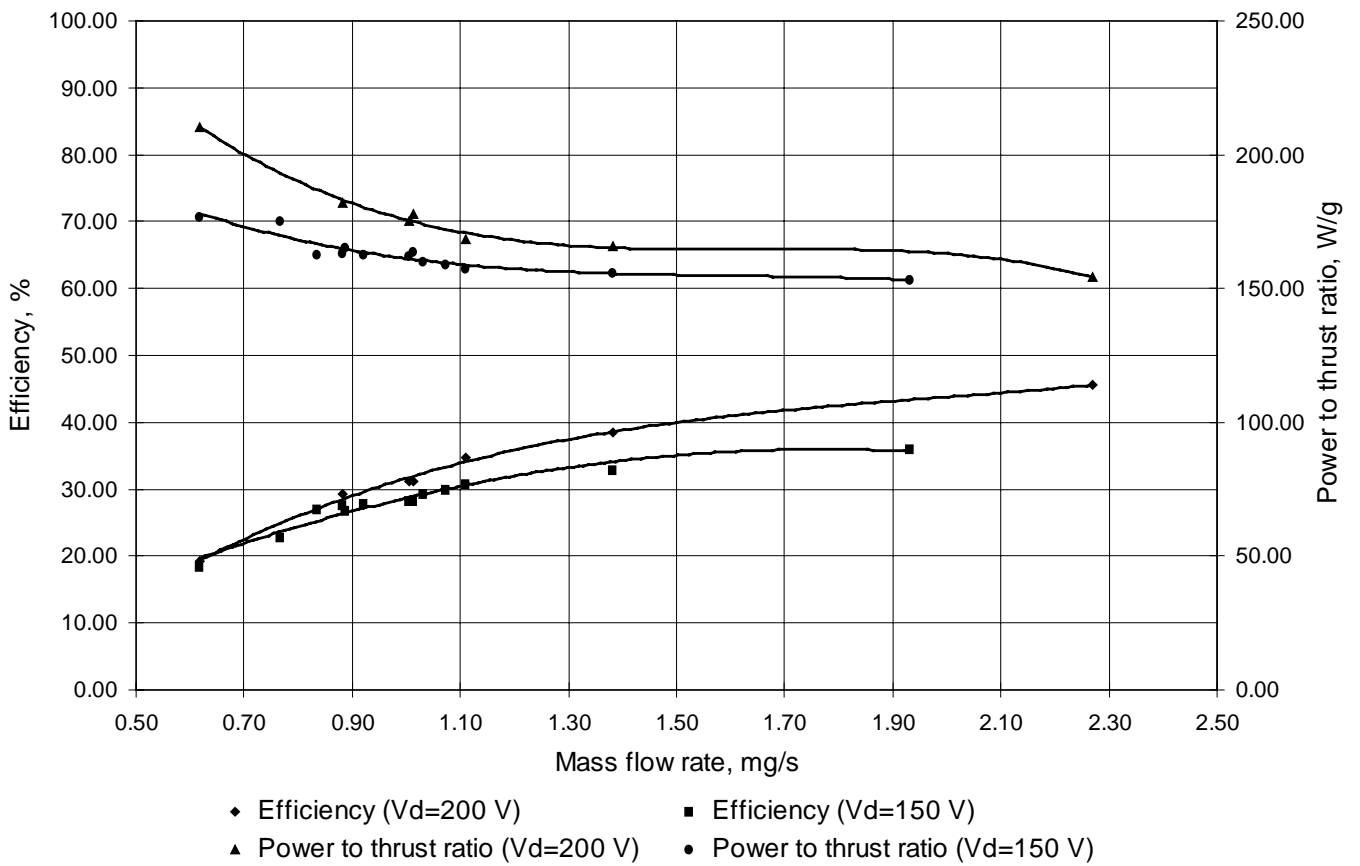
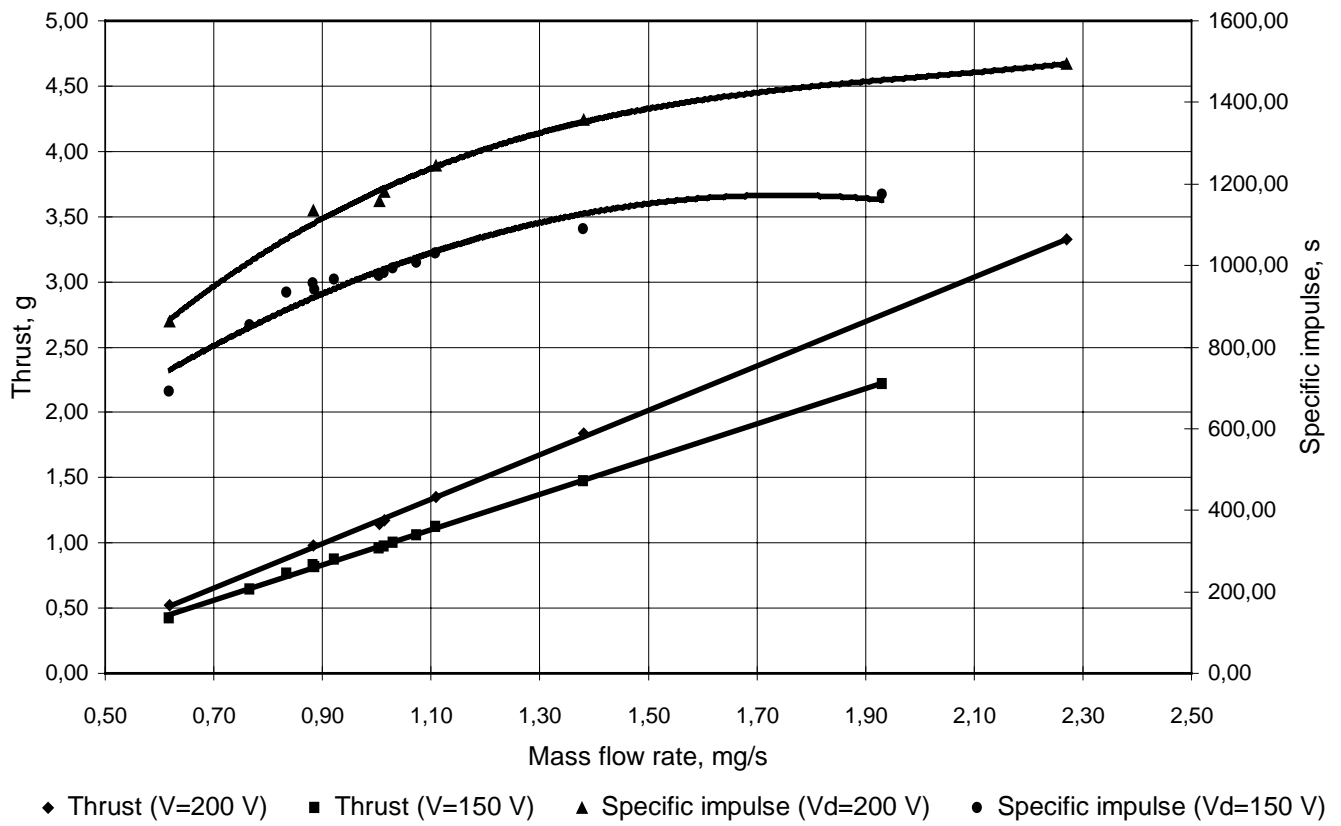


Fig. 19. Performances of D-38 thruster versus mass flow rate.

5. Discussion

To analyze influence of scaling factors, discussed above in Chapter 3, on characteristics of tested thrusters let us to compare their performances with D-55 thruster, which may be considered as good basis for such comparison. This thruster is convenient for comparative analysis because, on one hand, it is closest one to tested small thrusters. On another hand, it definitely has no scaling problems as compared with a bigger TALs of input power up to 50 kW, and working processes are one and the same for these thrusters at corresponding operation modes [3].

In Fig. 20 thrust, specific impulse and efficiency for D-38 and T-27 thrusters are plotted versus input discharge power together with the same data on the basic D-55 thruster had been thoroughly tested earlier in NASA LeRC and JPL during the joint work between NASA and TsNIIMASH [4].

Fig. 20 suggests that region of effective thruster operation tends to shift to lesser levels of propellant mass flow rate in accordance with characteristic thruster size. Smaller size provides higher xenon flow density and, correspondingly, allows to get effective ionization at smaller mass flows.

Ratio of mass flow to average anode diameter is a reasonable criteria for selection of comparable operating modes of thrusters with different size. But it is correct for the thrusters with identical geometry of discharge chamber. For our case it is not fully applicable, because of some differences in discharge chamber geometry of T-27, D-38, D-55.

As a criteria for comparison of the thrusters their efficiency and specific impulses at optimal operation regimes for each thruster - where efficiency value reaches the upper limit and is approximately constant with variation of mass flow - may be considered. For such regimes one can expect linear dependence of thrust versus discharge power also.

As it follows from Fig.20, for given discharge voltage (200V) efficiency and specific impulse of all three thrusters tend to one and the same level with increasing of discharge power, i. e. increasing of mass flow and, correspondingly, discharge current. For used regimes value of efficiency goes up to 0,45 and specific impulse – up to 1500 sec.

It is also important that the observed dependencies of thrust on input power (Fig.20) reserved their linearity being more inherent for higher input powers (Fig. 7).

Linearity of Thrust vs. Power dependencies and one and the same level of thrust efficiency for comparable regimes for all considering thrusters allow to say, that working processes are the same in all of them, and no essential negative influence on thruster operation was identified despite on significant variation of the thruster size.

This suggests that a physical limit at which the discussed above in Chapter 3 negative factors should noticeably disturb TAL working process, was not still reached even while operating the T-27 thruster, the smallest one of the tested thrusters. Therefore there is a reason to develop a new TAL version with further decreased average anode diameter and expected improvement of performance in low

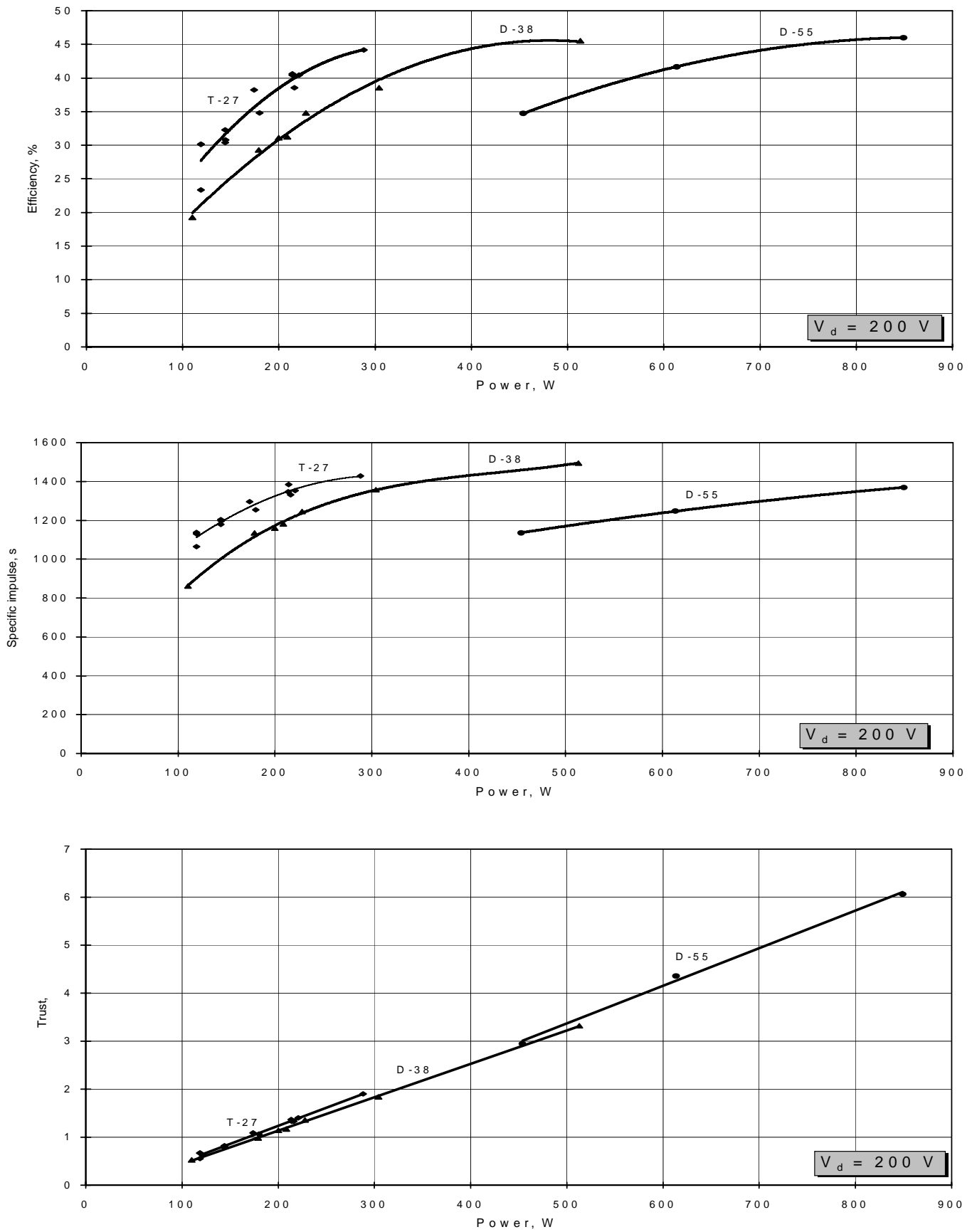


Fig. 20. Comparable characteristics of T-27, D-38 and D-55 thrusters.

input power range. Such development may be done with using available design methodologies and technical solutions, collected for thrusters with relatively high input power. And our consideration shows that these data base is applicable for the thruster with smaller size, than existing TALs.

The driving factor for reducing of size of low power thruster is efficiency of ionization processes. At the same time, as it was mentioned above, specially dedicated efforts never were made to get effective thruster operation at low propellant flow density and discharge voltage. So that, it is enough reasonable to perform such study in support of development of smaller thruster.

Miniaturization of the thruster may involve specific technological aspects also and simplification of the design is desirable. A preliminary consideration suggests that a perspective way to get it in regard of thruster magnetic system is use of permanent magnets instead of electrically driven ones. It is allow to simplify thruster cabling also and reduce total energy losses. It is important, that technologies and materials using for main TAL part – anode-gas distributor (typically- stainless steel), insulators (very wide spectrum of materials), metallic or graphite guard rings – do not have any difficulties in manufacturing and operation with small size and thickness, which are necessary for small low power thrusters with anode layer.

Based on performed consideration the following activity may be proposed as a continuation of low power TAL study and development at TsNIIMash:

1. Study of the possibility to update TAL design and increase ionization efficiency at low propellant flow densities and discharge voltage with using existing TAL hardware.
2. Elaboration of a new TAL version of smaller design size compared to existing ones to improve thruster performance in low input power range.

The latter may involve the first one as a risk reduction and supporting efforts and include several stages starting from conceptual design up to creation of a flight version for flight experiment.

Conclusion

1. Feasibility study of problems associated with development of thrusters with anode layer of 100...200 W range is performed. It is shown that decrease of dimensions and input power should be followed by enhancement of a number of scale factors reducing thruster's efficiency compared to that achieved on existing TALs at input powers greater than 500 W.
2. At TsNIIMASH facilities a demonstration test program was performed using existing TAL devices D-38 and D-27 in input power range from 100 to 500 W. The tested thrusters reserved effective operating mode in 100...200 W range of interest. For fixed 155 W operating mode the T-27 thruster exposed the best efficiency of 0,35 with thrust 1,05 G at specific impulse 1085 s. At input power 214 W the efficiency was risen to 0,41 with increase in thrust up to 1,37 G and in specific impulse to 1347 s.
3. An analysis of experimental data collected on available devices D-55, D-38 and T-27 in input power range from 100 to 1000 W suggests that a physical limit at which existing negative factors were expected to disturb TAL working process noticeably, was not reached even while operating the T-27 thruster, the smallest one of the thrusters tested. Therefore there is a reason to develop a new TAL version with further decreased average anode diameter and expected improvement of performance in low input power range.

References

1. V.Garkusha with col. Modern Status of Hall Thrusters Development in Russia AIAA 99-2157.
2. C.D. Grishin, L.V. Leskov. Electric Rocket Thrusters for Spacecraft. Moscow, "Engineering", 1989 (in Russian).
3. Alexander V. Semenkin, Sergey O. Tverdokhlebov, Valerii I. Garkusha, Sergey D. Grishin. TAL Thruster Technology for Advanced Electric Propulsion Systems. 20th International Symposium on Space Technology and Science. Gifu, Japan. May 19-25, 1996.
4. Operating characteristics of the Russian D-55 thruster with anode layer, AIAA-94-3011.
5. S.Tverdokhlebov. Study of Double-Stage Anode Layer Thruster Using Inert Gases, IEPC-93-232.
6. J.C. Dickens, Communications Impact of Hall Effect Plasma Thruster, PhD Thesis, Texas Tech University, 1996.
7. A.Semenkin, J. Yuen, C.Garner et al, Development Program and Preliminary Test Results of the TAL-110 Thruster, AIAA-99-2280.
8. P.Lynn, M.Osborn, I.Sankovic, L.Caveny. Electric Propulsion Demonstration Module (EPDM) Flight Thruster System, IEPC-97-100.
9. A.V. Semenkin with col. Performance Study of 4.5 kW Xenon Thruster with Anode Layer, IEPC-95-4.
10. C. Garner et al. Experimental evaluation of Russian Anode Layer Thruster, AIAA-94-3010.
11. A.V. Semenkin. Investigation of erosion in Anode Layer Thrusters and Elaboration High Life Design Scheme, IEPC-93-231.
12. B.S. Borisov et al. Experimental Study of Exhaust Beam of Anode Layer Thruster, IEPC-95-51.
13. Russian Patent 2030134 C1.
- 14 European Patent 0 778 415 A1.

Appendix

T-27 experimental results .

| Mass flow rate, mg/s | Discharge voltage, V | Discharge current, A | Power, W | Thrust, g | Efficiency, % | Power to thrust ratio, W/g | Specific impulse, s |
|----------------------|----------------------|----------------------|----------|-----------|---------------|----------------------------|---------------------|
| 0.53 | 91.7 | 0.57 | 52.27 | 0.27 | 12.16 | 196.84 | 508.82 |
| 0.53 | 100.0 | 0.55 | 55.00 | 0.29 | 14.14 | 187.21 | 562.95 |
| 0.53 | 120.0 | 0.54 | 64.80 | 0.38 | 19.56 | 172.80 | 718.57 |
| 0.53 | 140.0 | 0.54 | 75.60 | 0.45 | 23.96 | 168.65 | 858.98 |
| 0.53 | 149.0 | 0.55 | 81.95 | 0.47 | 24.50 | 173.65 | 904.28 |
| 0.53 | 160.5 | 0.56 | 89.88 | 0.50 | 25.14 | 179.51 | 959.42 |
| 0.53 | 170.0 | 0.58 | 98.60 | 0.51 | 23.98 | 192.50 | 981.47 |
| 0.53 | 180.0 | 0.59 | 106.20 | 0.53 | 23.79 | 200.58 | 1014.55 |
| 0.53 | 190.0 | 0.60 | 114.00 | 0.54 | 23.00 | 211.38 | 1033.45 |
| 0.53 | 198.0 | 0.60 | 118.80 | 0.55 | 23.37 | 214.08 | 1063.38 |
| 0.53 | 250.0 | 0.56 | 140.00 | 0.61 | 23.70 | 230.74 | 1162.63 |
| 0.53 | 301.0 | 0.56 | 168.56 | 0.68 | 24.59 | 248.55 | 1299.48 |
| 0.60 | 124.0 | 0.60 | 74.40 | 0.43 | 20.33 | 171.12 | 739.43 |
| 0.60 | 198.0 | 0.60 | 118.80 | 0.67 | 30.15 | 177.54 | 1137.99 |
| 0.61 | 125.0 | 0.59 | 73.75 | 0.43 | 19.78 | 171.73 | 722.24 |
| 0.61 | 150.0 | 0.59 | 88.50 | 0.54 | 26.38 | 162.92 | 913.56 |
| 0.61 | 151.0 | 0.59 | 89.09 | 0.52 | 24.22 | 170.60 | 878.26 |
| 0.61 | 198.0 | 0.60 | 118.80 | 0.67 | 30.15 | 176.57 | 1131.57 |
| 0.68 | 125.0 | 0.68 | 85.00 | 0.52 | 22.98 | 162.18 | 792.28 |
| 0.68 | 153.0 | 0.69 | 105.57 | 0.65 | 28.84 | 161.34 | 989.15 |
| 0.68 | 201.0 | 0.72 | 144.72 | 0.79 | 30.78 | 182.86 | 1196.39 |
| 0.68 | 103.0 | 0.69 | 71.07 | 0.38 | 14.30 | 186.85 | 567.82 |
| 0.68 | 125.0 | 0.68 | 85.00 | 0.51 | 21.42 | 166.93 | 760.15 |
| 0.68 | 200.0 | 0.72 | 144.00 | 0.79 | 30.37 | 182.47 | 1178.07 |
| 0.69 | 153.0 | 0.69 | 105.57 | 0.64 | 27.25 | 163.88 | 949.46 |
| 0.70 | 92.0 | 0.77 | 70.84 | 0.39 | 14.94 | 180.69 | 574.00 |
| 0.70 | 101.0 | 0.73 | 73.73 | 0.44 | 18.35 | 166.37 | 648.87 |
| 0.70 | 109.0 | 0.73 | 79.57 | 0.50 | 21.34 | 160.23 | 727.07 |
| 0.70 | 121.5 | 0.73 | 88.70 | 0.55 | 23.32 | 161.85 | 802.37 |
| 0.70 | 150.0 | 0.72 | 108.00 | 0.66 | 28.18 | 162.46 | 973.30 |
| 0.70 | 200.0 | 0.72 | 144.00 | 0.82 | 32.30 | 175.22 | 1203.27 |
| 0.70 | 251.0 | 0.80 | 200.80 | 0.98 | 32.74 | 205.52 | 1430.46 |
| 0.70 | 300.0 | 0.83 | 249.00 | 1.08 | 32.29 | 230.46 | 1581.92 |
| 0.86 | 130.0 | 0.91 | 118.30 | 0.77 | 27.78 | 154.30 | 911.19 |
| 0.86 | 200.0 | 0.87 | 174.00 | 1.09 | 38.20 | 159.58 | 1295.94 |
| 0.86 | 250.0 | 0.91 | 227.50 | 1.22 | 36.52 | 186.61 | 1448.91 |
| 0.86 | 300.0 | 0.91 | 273.00 | 1.37 | 38.48 | 199.16 | 1629.19 |
| 0.87 | 90.0 | 0.96 | 86.40 | 0.46 | 13.42 | 189.00 | 539.06 |
| 0.87 | 101.0 | 0.92 | 92.92 | 0.56 | 18.63 | 166.33 | 658.77 |
| 0.87 | 109.0 | 0.92 | 100.28 | 0.63 | 21.90 | 159.37 | 741.97 |
| 0.87 | 120.0 | 0.91 | 109.20 | 0.72 | 26.27 | 151.86 | 847.96 |
| 0.87 | 130.0 | 0.91 | 118.30 | 0.76 | 26.86 | 156.29 | 892.54 |

| | | | | | | | |
|------|-------|------|--------|------|-------|--------|---------|
| 0.87 | 140.0 | 0.90 | 126.00 | 0.82 | 29.43 | 154.09 | 964.20 |
| 0.87 | 150.0 | 0.90 | 135.00 | 0.89 | 32.28 | 152.31 | 1045.20 |
| 0.87 | 200.0 | 0.90 | 180.00 | 1.06 | 34.79 | 169.41 | 1252.89 |
| 0.87 | 250.0 | 0.95 | 237.50 | 1.24 | 35.68 | 192.16 | 1457.43 |
| 0.87 | 300.0 | 1.00 | 300.00 | 1.40 | 36.47 | 213.60 | 1656.17 |
| 0.98 | 202.0 | 1.06 | 214.12 | 1.33 | 40.41 | 161.14 | 1384.31 |
| 0.98 | 250.0 | 1.09 | 272.50 | 1.50 | 40.50 | 181.60 | 1563.31 |
| 0.98 | 302.0 | 1.15 | 347.30 | 1.73 | 42.22 | 200.79 | 1801.98 |
| 0.99 | 90.0 | 1.10 | 99.00 | 0.58 | 16.37 | 171.35 | 596.28 |
| 0.99 | 100.0 | 1.10 | 110.00 | 0.68 | 20.52 | 161.33 | 703.66 |
| 0.99 | 110.0 | 1.07 | 117.70 | 0.76 | 24.08 | 154.05 | 788.52 |
| 0.99 | 121.0 | 1.05 | 127.05 | 0.86 | 28.40 | 147.38 | 889.68 |
| 0.99 | 150.0 | 1.03 | 154.50 | 1.05 | 34.72 | 146.98 | 1084.80 |
| 0.99 | 251.0 | 1.02 | 256.02 | 1.49 | 42.02 | 171.98 | 1536.31 |
| 0.99 | 300.0 | 1.08 | 324.00 | 1.60 | 38.19 | 202.93 | 1647.73 |
| 1.02 | 149.6 | 1.06 | 158.58 | 1.03 | 31.56 | 153.86 | 1032.23 |
| 1.02 | 200.0 | 1.08 | 216.00 | 1.33 | 38.54 | 162.50 | 1331.28 |
| 1.04 | 124.0 | 1.09 | 135.16 | 0.85 | 24.46 | 159.82 | 830.98 |
| 1.04 | 124.0 | 1.11 | 137.64 | 0.85 | 24.42 | 161.41 | 837.94 |
| 1.04 | 156.0 | 1.05 | 163.80 | 1.06 | 31.81 | 154.28 | 1043.27 |
| 1.04 | 203.6 | 1.05 | 213.78 | 1.37 | 40.60 | 156.00 | 1346.55 |
| 1.04 | 250.0 | 1.05 | 262.50 | 1.57 | 43.43 | 167.14 | 1543.25 |
| 1.06 | 80.0 | 1.50 | 120.00 | 0.44 | 7.26 | 273.85 | 422.85 |
| 1.06 | 92.0 | 1.42 | 130.64 | 0.63 | 14.00 | 205.79 | 612.59 |
| 1.06 | 100.0 | 1.17 | 117.00 | 0.69 | 18.23 | 170.70 | 661.38 |
| 1.06 | 110.0 | 1.16 | 127.60 | 0.80 | 22.64 | 159.95 | 769.80 |
| 1.06 | 120.0 | 1.14 | 136.80 | 0.90 | 27.11 | 151.36 | 872.16 |
| 1.06 | 150.0 | 1.12 | 168.00 | 1.14 | 34.84 | 147.94 | 1095.79 |
| 1.06 | 199.0 | 1.11 | 220.89 | 1.40 | 40.40 | 157.54 | 1352.96 |
| 1.35 | 81.0 | 1.30 | 105.30 | 0.55 | 10.29 | 190.71 | 417.34 |
| 1.35 | 100.0 | 1.51 | 151.00 | 0.80 | 15.21 | 187.89 | 607.47 |
| 1.35 | 102.0 | 1.54 | 157.08 | 0.87 | 17.03 | 181.08 | 655.68 |
| 1.35 | 126.0 | 1.54 | 194.04 | 1.25 | 28.63 | 155.23 | 944.82 |
| 1.35 | 152.0 | 1.46 | 221.92 | 1.49 | 35.76 | 148.55 | 1129.18 |
| 1.36 | 203.0 | 1.42 | 288.26 | 1.90 | 44.19 | 151.91 | 1427.14 |
| 1.36 | 251.0 | 1.43 | 358.93 | 2.30 | 52.16 | 156.02 | 1730.16 |

T-27 demonstration test results (TsNIIMash, 14/10/99 and 15/10/99)

| Mass flow rate, mg/s | Discharge voltage, V | Discharge current, A | Power, W | Thrust, g | Efficiency, % | Power to thrust ratio, W/g | Specific impulse, s |
|----------------------|----------------------|----------------------|----------|-----------|---------------|----------------------------|---------------------|
| 0.89 | 150 | 0.95 | 143 | 0.99 | 0.371 | 0.144 | 1.110 |
| 0.89 | 202 | 0.95 | 192 | 1.28 | 0.457 | 0.150 | 1.431 |
| 0.89 | 298 | 0.98 | 292 | 1.65 | 0.499 | 0.177 | 1.844 |
| 0.89 | 126 | 0.98 | 123 | 0.88 | 0.337 | 0.140 | 0.985 |
| 0.96 | 152 | 0.99 | 150 | 1.06 | 0.374 | 0.142 | 1.106 |
| 0.96 | 123 | 1.03 | 127 | 0.84 | 0.280 | 0.150 | 0.878 |
| 0.96 | 100 | 1.03 | 103 | 0.46 | 0.103 | 0.224 | 0.479 |

D-38 experimental results .

| Mass flow rate, mg/s | Discharge voltage, V | Discharge current, A | Power, W | Thrust, g | Efficiency, % | Power to thrust ratio, W/g | Specific impulse, s |
|----------------------|----------------------|----------------------|----------|-----------|---------------|----------------------------|---------------------|
| 0.62 | 122.7 | 0.49 | 60.12 | 0.34 | 14.67 | 178.30 | 555.91 |
| 0.62 | 148.3 | 0.50 | 74.15 | 0.42 | 18.41 | 176.74 | 691.64 |
| 0.62 | 200.0 | 0.55 | 110.00 | 0.52 | 19.28 | 210.33 | 862.18 |
| 0.62 | 250.0 | 0.55 | 137.50 | 0.59 | 19.76 | 232.28 | 975.88 |
| 0.62 | 300.5 | 0.55 | 165.28 | 0.68 | 21.58 | 243.71 | 1117.99 |
| 0.77 | 100.5 | 0.68 | 68.34 | 0.41 | 15.03 | 168.69 | 538.90 |
| 0.77 | 125.5 | 0.72 | 90.36 | 0.54 | 20.21 | 167.28 | 718.53 |
| 0.77 | 150.0 | 0.75 | 112.50 | 0.64 | 22.89 | 175.38 | 853.26 |
| 0.84 | 129.0 | 0.84 | 108.36 | 0.66 | 23.17 | 163.92 | 807.44 |
| 0.84 | 150.0 | 0.83 | 124.50 | 0.77 | 27.04 | 162.67 | 934.89 |
| 0.88 | 68.5 | 0.90 | 61.65 | 0.23 | 4.70 | 267.05 | 266.75 |
| 0.88 | 81.0 | 0.85 | 68.85 | 0.37 | 10.57 | 188.12 | 422.90 |
| 0.88 | 90.0 | 0.84 | 75.60 | 0.46 | 15.33 | 163.74 | 533.51 |
| 0.88 | 99.0 | 0.85 | 84.15 | 0.52 | 17.44 | 161.97 | 600.35 |
| 0.88 | 109.0 | 0.86 | 93.74 | 0.59 | 20.30 | 158.44 | 683.65 |
| 0.88 | 120.0 | 0.90 | 108.00 | 0.67 | 22.79 | 160.51 | 777.49 |
| 0.88 | 129.0 | 0.90 | 116.10 | 0.71 | 23.83 | 162.73 | 824.40 |
| 0.88 | 130.0 | 0.90 | 117.00 | 0.73 | 24.42 | 161.37 | 837.81 |
| 0.88 | 140.0 | 0.91 | 127.40 | 0.77 | 25.39 | 165.14 | 891.43 |
| 0.88 | 150.0 | 0.90 | 135.00 | 0.83 | 27.63 | 162.96 | 957.22 |
| 0.88 | 160.0 | 0.90 | 144.00 | 0.86 | 27.89 | 167.51 | 993.33 |
| 0.88 | 170.0 | 0.90 | 153.00 | 0.89 | 28.07 | 172.13 | 1027.11 |
| 0.88 | 180.0 | 0.90 | 162.00 | 0.92 | 28.28 | 176.45 | 1060.90 |
| 0.88 | 199.0 | 0.90 | 179.10 | 0.98 | 29.31 | 182.26 | 1135.47 |
| 0.88 | 250.0 | 0.88 | 220.00 | 1.16 | 33.02 | 190.30 | 1335.84 |
| 0.88 | 300.0 | 0.90 | 270.00 | 1.29 | 33.75 | 208.53 | 1496.14 |
| 0.89 | 100.0 | 0.87 | 87.00 | 0.54 | 18.26 | 160.63 | 623.37 |
| 0.89 | 130.0 | 0.91 | 118.30 | 0.73 | 24.15 | 162.85 | 836.10 |
| 0.89 | 150.0 | 0.90 | 135.00 | 0.82 | 26.79 | 165.19 | 940.61 |
| 0.92 | 100.0 | 0.92 | 92.00 | 0.58 | 18.94 | 158.99 | 640.21 |
| 0.92 | 130.0 | 0.96 | 124.80 | 0.78 | 25.13 | 160.78 | 858.78 |
| 0.92 | 149.5 | 0.95 | 142.03 | 0.87 | 27.90 | 162.78 | 965.35 |
| 1.01 | 140.0 | 1.04 | 145.60 | 0.91 | 26.98 | 160.53 | 920.65 |
| 1.01 | 150.0 | 1.04 | 156.00 | 0.96 | 28.30 | 162.22 | 976.12 |
| 1.01 | 160.0 | 1.03 | 164.80 | 1.01 | 29.32 | 163.83 | 1021.08 |
| 1.01 | 170.0 | 1.02 | 173.40 | 1.04 | 29.87 | 166.50 | 1057.12 |
| 1.01 | 180.0 | 1.02 | 183.60 | 1.05 | 28.48 | 175.44 | 1062.29 |
| 1.01 | 190.0 | 1.01 | 191.90 | 1.13 | 31.74 | 169.91 | 1146.44 |
| 1.01 | 200.0 | 1.00 | 200.00 | 1.14 | 31.09 | 175.26 | 1158.38 |
| 1.01 | 250.0 | 0.98 | 245.00 | 1.31 | 33.46 | 186.97 | 1330.10 |
| 1.01 | 301.0 | 0.99 | 297.99 | 1.49 | 35.78 | 199.42 | 1516.78 |
| 1.01 | 60.0 | 0.69 | 41.40 | 0.16 | 3.02 | 255.05 | 163.86 |
| 1.01 | 69.0 | 1.07 | 73.83 | 0.33 | 7.02 | 223.43 | 333.58 |

| | | | | | | | |
|------|-------|------|--------|------|-------|--------|---------|
| 1.01 | 80.0 | 0.99 | 79.20 | 0.42 | 10.55 | 188.78 | 423.53 |
| 1.01 | 91.0 | 0.94 | 85.54 | 0.52 | 14.91 | 165.04 | 523.22 |
| 1.01 | 100.0 | 0.96 | 96.00 | 0.62 | 18.85 | 155.52 | 623.16 |
| 1.01 | 110.0 | 0.98 | 107.80 | 0.69 | 20.80 | 156.88 | 693.70 |
| 1.01 | 120.0 | 1.01 | 121.20 | 0.78 | 23.86 | 155.32 | 787.77 |
| 1.01 | 125.0 | 1.02 | 127.50 | 0.81 | 24.40 | 157.51 | 817.16 |
| 1.01 | 130.0 | 1.03 | 133.90 | 0.84 | 25.29 | 158.57 | 852.43 |
| 1.01 | 90.5 | 0.95 | 85.98 | 0.52 | 15.10 | 164.17 | 527.15 |
| 1.01 | 100.5 | 0.96 | 96.48 | 0.63 | 19.24 | 154.09 | 630.29 |
| 1.01 | 126.0 | 1.03 | 129.78 | 0.82 | 24.51 | 158.33 | 825.10 |
| 1.01 | 150.5 | 1.06 | 159.53 | 0.97 | 28.19 | 163.70 | 980.96 |
| 1.01 | 200.5 | 1.04 | 208.52 | 1.17 | 31.22 | 177.83 | 1180.35 |
| 1.01 | 250.0 | 1.00 | 250.00 | 1.36 | 35.17 | 183.47 | 1371.61 |
| 1.01 | 300.0 | 1.00 | 300.00 | 1.54 | 37.23 | 195.34 | 1545.97 |
| 1.03 | 80.0 | 1.03 | 82.40 | 0.45 | 11.50 | 182.72 | 446.61 |
| 1.03 | 88.0 | 1.00 | 88.00 | 0.56 | 16.41 | 158.04 | 551.45 |
| 1.03 | 100.0 | 1.00 | 100.00 | 0.66 | 20.59 | 150.43 | 658.37 |
| 1.03 | 109.0 | 1.02 | 111.18 | 0.73 | 22.20 | 152.74 | 720.87 |
| 1.03 | 125.0 | 1.05 | 131.25 | 0.85 | 25.37 | 155.24 | 837.32 |
| 1.03 | 130.0 | 1.07 | 139.10 | 0.90 | 26.84 | 155.39 | 886.56 |
| 1.03 | 140.0 | 1.07 | 149.80 | 0.95 | 28.18 | 157.38 | 942.67 |
| 1.03 | 150.0 | 1.07 | 160.50 | 1.00 | 29.19 | 160.05 | 993.17 |
| 1.07 | 80.0 | 1.10 | 88.00 | 0.49 | 12.42 | 178.00 | 469.89 |
| 1.07 | 99.6 | 1.04 | 103.58 | 0.70 | 21.22 | 147.74 | 666.40 |
| 1.07 | 130.0 | 1.13 | 146.90 | 0.93 | 26.25 | 158.17 | 882.76 |
| 1.07 | 149.0 | 1.13 | 168.37 | 1.06 | 29.83 | 158.87 | 1007.32 |
| 1.11 | 80.0 | 1.12 | 89.60 | 0.49 | 11.83 | 181.05 | 455.28 |
| 1.11 | 90.0 | 1.07 | 96.30 | 0.61 | 16.96 | 156.76 | 565.18 |
| 1.11 | 102.0 | 1.07 | 109.14 | 0.74 | 21.68 | 147.59 | 680.31 |
| 1.11 | 110.0 | 1.07 | 117.70 | 0.80 | 23.65 | 146.75 | 737.87 |
| 1.11 | 127.5 | 1.13 | 144.08 | 0.94 | 26.78 | 152.58 | 868.70 |
| 1.11 | 142.0 | 1.16 | 164.72 | 1.06 | 29.41 | 155.69 | 973.37 |
| 1.11 | 152.0 | 1.16 | 176.32 | 1.12 | 30.82 | 157.35 | 1030.93 |
| 1.11 | 162.0 | 1.15 | 186.30 | 1.15 | 30.97 | 161.34 | 1062.33 |
| 1.11 | 200.0 | 1.14 | 228.00 | 1.35 | 34.83 | 168.31 | 1246.26 |
| 1.11 | 250.0 | 1.10 | 275.00 | 1.55 | 37.65 | 177.79 | 1422.98 |
| 1.11 | 301.0 | 1.10 | 331.10 | 1.72 | 38.77 | 192.23 | 1584.57 |
| 1.38 | 91.5 | 1.46 | 133.59 | 0.86 | 19.44 | 154.54 | 638.65 |
| 1.38 | 100.5 | 1.40 | 140.70 | 0.95 | 22.06 | 148.87 | 698.26 |
| 1.38 | 125.5 | 1.40 | 175.70 | 1.22 | 29.52 | 143.81 | 902.63 |
| 1.38 | 151.5 | 1.52 | 230.28 | 1.48 | 32.85 | 156.09 | 1089.96 |
| 1.38 | 201.5 | 1.51 | 304.27 | 1.84 | 38.55 | 165.61 | 1357.31 |
| 1.38 | 250.5 | 1.41 | 353.21 | 2.06 | 41.93 | 171.11 | 1525.03 |
| 1.38 | 300.5 | 1.41 | 423.71 | 2.32 | 44.01 | 182.91 | 1711.42 |
| 1.93 | 95.0 | 2.23 | 211.85 | 1.32 | 20.53 | 160.17 | 699.01 |
| 1.93 | 103.5 | 2.18 | 225.63 | 1.51 | 24.96 | 149.91 | 795.43 |
| 1.93 | 123.5 | 2.19 | 270.47 | 1.82 | 30.38 | 148.76 | 960.87 |

| | | | | | | | |
|------|-------|------|--------|------|-------|--------|---------|
| 1.93 | 150.5 | 2.26 | 340.13 | 2.22 | 36.05 | 153.15 | 1173.71 |
| 1.93 | 250.5 | 2.02 | 506.01 | 3.09 | 46.97 | 163.64 | 1634.15 |
| 1.93 | 300.0 | 2.02 | 606.00 | 3.44 | 48.61 | 176.05 | 1819.15 |
| 2.27 | 124.0 | 2.70 | 334.80 | 2.19 | 30.15 | 153.20 | 982.07 |
| 2.27 | 153.5 | 2.79 | 428.27 | 2.70 | 35.99 | 158.60 | 1213.45 |
| 2.27 | 202.0 | 2.54 | 513.08 | 3.33 | 45.57 | 154.28 | 1494.47 |
| 2.27 | 250.5 | 2.48 | 621.24 | 3.97 | 53.54 | 156.62 | 1782.56 |
| 2.27 | 302.0 | 2.46 | 742.92 | 4.46 | 56.71 | 166.41 | 2006.19 |

D-38 demonstration test results (TsNIIMash, 12/10/99)

| Mass flow rate, mg/s | Discharge voltage, V | Discharge current, A | Power, W | Thrust, g | Efficiency, % | Power to thrust ratio, W/g | Specific impulse, s |
|----------------------|----------------------|----------------------|----------|-----------|---------------|----------------------------|---------------------|
| 2.11 | 300 | 2.25 | 675 | — | — | — | — |
| 2.11 | 300 | 2.25 | 675 | 4.22 | 0.600 | 0.160 | 1.997 |
| 2.11 | 250 | 2.26 | 565 | 3.58 | 0.516 | 0.158 | 1.695 |
| 2.11 | 202 | 2.39 | 483 | 3.03 | 0.432 | 0.159 | 1.433 |
| 2.11 | 154 | 2.55 | 392 | 2.36 | 0.322 | 0.166 | 1.115 |
| 2.11 | 124 | 2.46 | 305 | 1.91 | 0.271 | 0.160 | 0.903 |
| 2.11 | 100 | 2.61 | 261 | — | — | — | — |
| 2.11 | 75 | 2.20 | 165 | — | — | — | — |
| 1.42 | 300 | 1.54 | 462 | 2.22 | 0.361 | 0.208 | 1.566 |
| 1.42 | 250 | 1.57 | 393 | 1.95 | 0.329 | 0.201 | 1.378 |
| 1.42 | 200 | 1.60 | 320 | 1.87 | 0.369 | 0.171 | 1.316 |
| 1.42 | 150 | 1.63 | 245 | 1.44 | 0.288 | 0.169 | 1.017 |
| 1.42 | 125 | 1.53 | 191 | 1.27 | 0.286 | 0.150 | 0.896 |
| 1.42 | 100 | 1.61 | 161 | 0.72 | 0.109 | 0.223 | 0.509 |
| 1.07 | 300 | 1.14 | 342 | 1.78 | 0.419 | 0.192 | 1.674 |
| 1.07 | 200 | 1.14 | 228 | 1.31 | 0.336 | 0.175 | 1.225 |
| 1.07 | 150 | 1.15 | 173 | 1.05 | 0.289 | 0.164 | 0.987 |
| 1.07 | 125 | 1.09 | 136 | 0.73 | 0.178 | 0.186 | 0.688 |
| 1.07 | 100 | 1.11 | 111 | 0.35 | 0.051 | 0.313 | 0.333 |